Cell Reports

Pre-existing immunity modulates responses to mRNA boosters

Graphical abstract
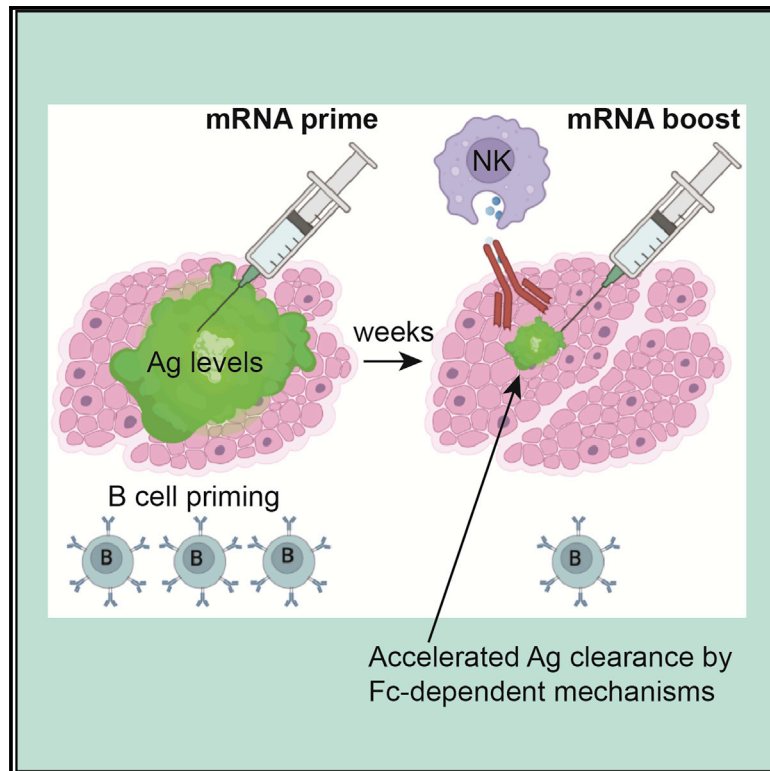
Authors

Tanushree Dangi, Sarah Sanchez,
Min Han Lew, ..., Justin M. Richner,
Igor J. Koralnik,
Pablo Penaloza-MacMaster

Correspondence

ppm@northwestern.edu

In brief

Dangi et al. show that pre-existing antibodies accelerate the clearance of vaccine antigen via Fc-dependent mechanisms, limiting the amount of antigen available to prime B cell responses after mRNA boosters. This finding suggests that transient downmodulation of antibody effector mechanisms may improve the serial re-utilization of mRNA-LNPs.

Highlights

- Low antibody before boost is correlated with high fold-increase in antibody

- Pre-existing antibody accelerates clearance of vaccine antigen after vaccination

- Accelerated clearance of vaccine antigen limits B cell priming after vaccination

- Pre-existing HIV-specific antibody limits responses by an mRNA-HIV vaccine

CelPress

Article

Pre-existing immunity modulates responses to mRNA boosters

Tanushree Dangi,[1] Sarah Sanchez,[1] Min Han Lew,[1] Bakare Awakoaiye,[1] Lavanya Visvabharathy,[2] Justin M. Richner,[3] Igor J. Koralnik,[2] and Pablo Penaloza-MacMaster[1,4,*]

[1]Department of Microbiology-Immunology, Feinberg School of Medicine, Northwestern University, Chicago, IL 60611, USA
[2]Ken and Ruth Davee Department of Neurology, Feinberg School of Medicine, Northwestern University, Chicago, IL 60611, USA
[3]Department of Microbiology and Immunology, University of Illinois Chicago College of Medicine, Chicago, IL 60612, USA
[4]Lead contact
*Correspondence: ppm@northwestern.edu
https://doi.org/10.1016/j.celrep.2023.112167

SUMMARY

mRNA vaccines are effective in preventing severe COVID-19, but breakthrough infections, emerging variants, and waning immunity warrant the use of boosters. Although mRNA boosters are being implemented, the extent to which pre-existing immunity influences the efficacy of boosters remains unclear. In a cohort of individuals primed with the mRNA-1273 or BNT162b2 vaccines, we report that lower antibody levels before boost are associated with higher fold-increase in antibody levels after boost, suggesting that pre-existing antibody modulates the immunogenicity of mRNA vaccines. Our studies in mice show that pre-existing antibodies accelerate the clearance of vaccine antigen via Fc-dependent mechanisms, limiting the amount of antigen available to prime B cell responses after mRNA boosters. These data demonstrate a "tug of war" between pre-existing antibody responses and de novo B cell responses following mRNA vaccination, and they suggest that transient downmodulation of antibody effector function may improve the efficacy of mRNA boosters.

INTRODUCTION

mRNA lipid nanoparticle (mRNA-LNP) vaccines have been administered to millions of people, showing high efficacy against COVID-19. Despite their wide use, the immunobiology of mRNA-LNPs remains incompletely understood, and it is unclear whether pre-existing immunity elicited by prior immunizations affects the re-utilization of mRNA-LNPs. This knowledge would be critical during the current phase of the COVID-19 pandemic, as updated boosters are used. Both Pfizer-BioNTech and Moderna have deployed their updated mRNA boosters. Moderna released preliminary data on its phase 2/3 trial (ClinicalTrials.gov: NCT05249829), which suggested that an updated bivalent booster based on both Omicron and ancestral spike antigens elicits superior neutralizing antibody against Omicron than the ancestral vaccine. Other studies have suggested that when given as a third shot, Omicron vaccines do not confer a substantial improvement in the immune response against Omicron relative to the original vaccine, suggesting that pre-existing immunity modulates responses to boosters.[1,2] In the present study, we aimed to answer two critical questions. First, how does pre-existing immunity affect responses to mRNA boosters? Second, are there specific circumstances where updated vaccines are more effective than ancestral vaccines? We show that pre-existing antibodies can impinge on the efficacy of mRNA vaccines via antibody effector functions, and that the relative superiority of a monovalent Omicron vaccine depends on the serostatus of the host. These data provide insights for next-generation mRNA vaccines.

RESULTS

Lower pre-boost antibody levels are associated with higher fold-increase in post-boost antibody levels

Despite effective vaccines, SARS-CoV-2 continues to spread worldwide. This has motivated administering additional boosters, but little is known about how pre-existing immunity affects responses elicited by boosters. We first interrogated whether the level of pre-existing immunity to SARS-CoV-2 affects the boosting capacity of mRNA vaccines in a cohort of unexposed (COVID-19 negative) individuals who previously received one dose of the Pfizer-BioNTech or Moderna mRNA vaccines (Figure S1A). Interestingly, volunteers who exhibited the lowest spike-specific antibody response before boost showed the highest fold-increase in spike-specific antibody after boost (Figure S1B).

We also analyzed a cohort of individuals with prior SARS-CoV-2 infection, and we observed that individuals with the lowest antibody responses following infection (pre-vaccination) showed the highest fold-increase in antibody responses after the first vaccine dose (Figures S1C and S1D, red data points). A similar inverse association was observed in SARS-CoV-2 convalescent individuals who received a second vaccine dose (Figures S1C and S1E, blue data points; Table S1). The boosting still conferred an immunological benefit, because it increased the overall antibody titers in all volunteers, but the data suggested that as antibody responses plateau, it becomes increasingly more difficult to boost those responses. Collectively, these data demonstrate an inverse association between pre-existing
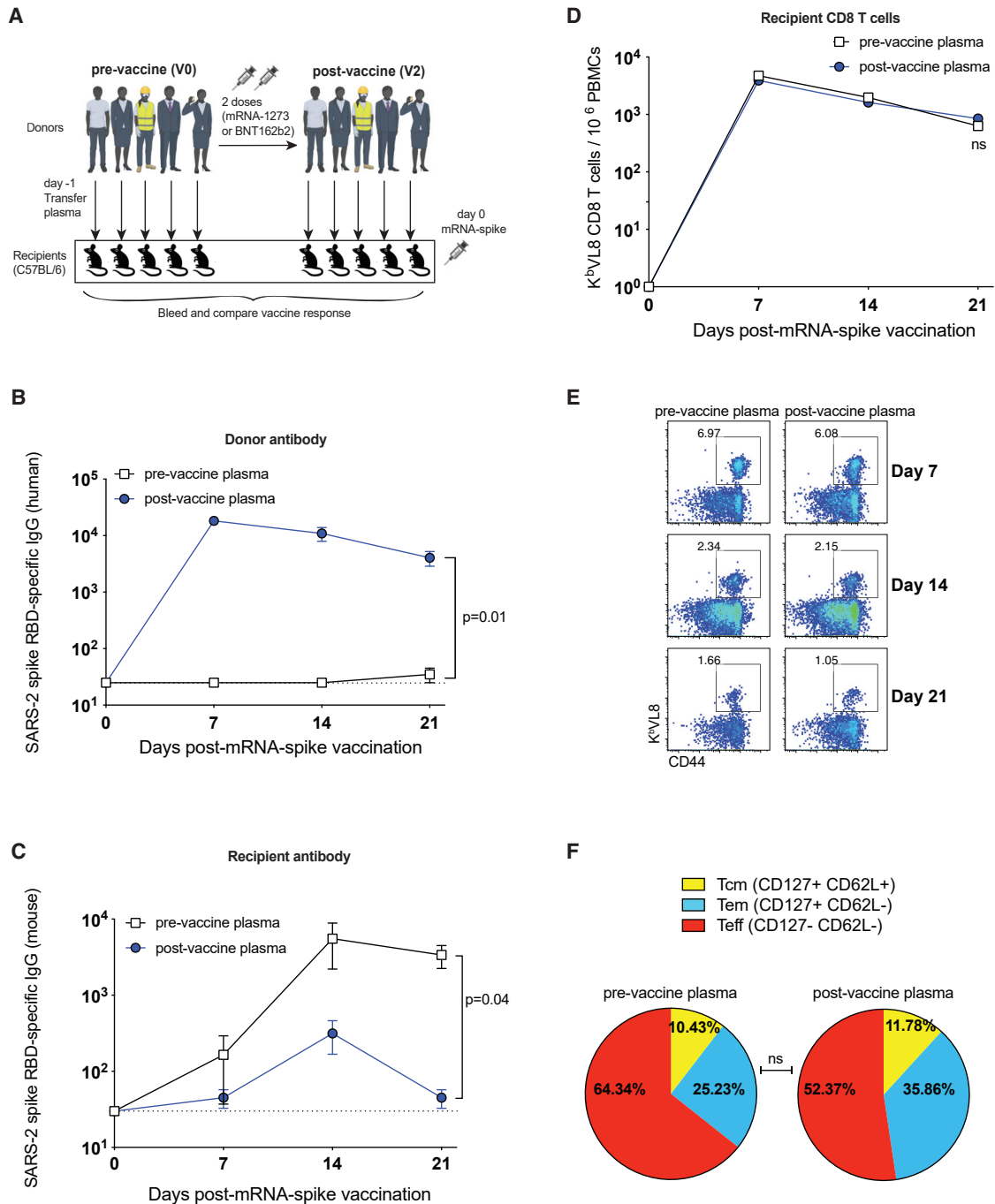
Figure 1. Plasma from mRNA-1273- or BNT162b2-vaccinated humans abrogates *de novo* antibody responses following mRNA vaccination

(A) Experimental layout. Donor-matched plasmas were harvested from five different human donors; pre-vaccination (V0) and post-vaccination (V2 corresponding to 2–3 weeks after second dose). A total of 100 μL of these donor-matched human plasmas was adoptively transferred via the intraperitoneal route into C57BL/6 mice. On the following day, all mice were immunized intramuscularly with 3 μg of an mRNA expressing SARS-CoV-2 spike, and immune responses were quantified longitudinally.

(B) Donor (human-derived) SARS-CoV-2 spike RBD-specific antibody in recipient mice.

(C) *De novo* (mouse-derived) SARS-CoV-2 spike RBD-specific antibody in recipient mice.

(D) Summary of SARS-CoV-2 spike-specific CD8 T cells.

(E) Representative FACS plots of SARS-CoV-2 spike-specific CD8 T cells. FACS plots are gated on live CD8 T cells.

(legend continued on next page)

antibody levels and the ability of mRNA vaccines to boost antibody responses. To better understand the mechanism of how seropositivity affects responses to mRNA vaccines, we performed passive immunization studies in mice.

Immune plasma from mRNA-1273- or BNT162b2-vaccinated individuals abrogates *de novo* priming of B cell responses

Our data from vaccinated humans suggested that pre-existing antibody to the vaccine antigen (SARS-CoV-2 spike) downmodulates immune responses following booster vaccination. To evaluate the effect of pre-existing humoral responses on mRNA vaccines, we transferred donor-matched human plasma (pre-vaccination and post-vaccination plasma) into naive C57BL/6 mice, and on the following day, recipient mice received an mRNA vaccine expressing the SARS-CoV-2 spike protein (mRNA-spike) (Figure 1A). Human- and mouse-derived antibodies were distinguished using host-specific enzyme-linked immunosorbent assays (ELISAs), allowing us to track donor-derived and recipient-derived antibodies over time.

We were able to detect human spike-specific antibody in all mice that received post-vaccination plasma (Figure 1B). Interestingly, mice that received post-vaccination human plasma showed a significant impairment in *de novo* antibody responses (Figure 1C). We did not observe any significant differences in the levels of CD8 T cells (Figure 1D) or their memory differentiation (Figures 1E and 1F). In another experiment, we transferred plasma from a different set of human donors with escalating levels of spike-specific antibody (after additional boosting) (Figure 2A). Mice that received plasma with high titer of spike-specific antibodies (after three vaccine shots) showed the lowest *de novo* antibody response (Figures 2B and 2C). These data suggested that antibodies elicited by prior mRNA vaccinations negatively affect primary antibody responses during an mRNA booster, and that such effect was dose dependent.

Following a booster immunization, both primary and secondary B cell responses can be recruited to the immune response.[3] We devised an experimental model that allowed us to track primary B cell responses using the same donor and recipient animal species (Figure 3A). We first primed C57BL/6 mice with mRNA-spike and then boosted these mice at week 3 to generate high levels of spike-specific antibodies. At week 2 post-boost, we harvested immune plasma from these vaccinated mice and transferred it into naive recipient BALB/c mice. On the following day, the recipient mice were immunized with the mRNA-spike vaccine, and immune responses were measured. Note that donor-derived and recipient-derived antibodies can be distinguished based on their immunoglobulin allotype. Antibodies from donor C57BL/6 mice contain an IgG1[b] allotype, whereas antibodies from recipient BALB/c mice contain an IgG1[a] allotype. These two allotypes can be distinguished using allotype-specific ELISAs, allowing us to independently track donor-derived and recipient-derived antibodies over time.

As expected, donor spike-specific antibody was detectable in recipient mice that received spike-immune plasma (Figure 3B), and these mice showed significantly impaired antibody responses to the spike protein (Figure 3C), as well as the receptor binding domain (RBD; Figure 3D), consistent with our data with human plasma transfer. These data demonstrate that seropositivity to the vaccine antigen significantly impairs *de novo* antibody responses following mRNA vaccination. Plasma contains various molecules besides antibodies, so we interrogated the specific role of IgG antibodies. We purified IgG from the plasma of mRNA-spike immune mice using a protein G column and then transferred purified IgG into naive recipient mice, followed by mRNA-spike vaccination (Figure S2A). Spike-specific donor-derived IgG was detected in recipient mice (Figure S2B), and it limited the elicitation of spike-specific antibody responses in recipient mice (Figure S2C).

After immunization, long-term humoral immunity is maintained by a subset of B cells that reside mostly in the bone marrow, known as plasma cells.[4,5] We quantified plasma cells at week 3 post-immunization using an ELISPOT-based antibody-secreting cell assay (Figure 3E), and we observed an 8-fold reduction in the number of vaccine-induced plasma cells in mice that received immune plasma (Figure 3F). A single shot of vaccine generated low numbers of splenic memory B cells (MBCs) in mice that received naive plasma, but there were no detectable MBCs in mice that received immune plasma (Figures 3G and 3H). In addition, mice that received immune plasma were not able to generate cross-reactive Omicron-specific antibodies (Figure 3I). Taken together, pre-existing antibodies significantly curtail *de novo* generation of B cell responses following mRNA vaccination.

Effects of pre-existing immunity on Omicron-based vaccines

As the human population reaches immunity to SARS-CoV-2 either by vaccination or infection, it becomes important to understand the effects of pre-existing immunity on vaccine boosters. Recently, the new Omicron (B.1.1.529) variant was identified and is now prevalent worldwide. Due to its high number of mutations, Omicron can evade antibody responses elicited by ancestral vaccines, motivating the development of Omicron-based boosters, but it remains unclear how pre-existing immunity affects the response to updated boosters. A recent study evaluated the effect of a "third shot" with an Omicron vaccine in animals that were initially primed and boosted with the ancestral vaccine.[2] This prior study showed that when given as a third shot, an Omicron vaccine elicits comparable antibody responses relative to an ancestral vaccine. Because a fraction of the human population has received only one vaccine dose, it would be important to understand the effect of Omicron vaccines when given as a second shot. One can reason that the effect of an Omicron booster may differ in the context of a second shot versus a third shot, because the level of pre-existing immunity increases after each additional booster.

(F) Summary of memory markers on K[b]VL8^{+} CD8 T cells at day 21 post-vaccination. Two-tailed parametric test (matched) was used. Data are from an experiment with five mice that received pre-vaccine human plasma and five mice that received post-vaccine human plasma (donor-matched); data from all experiments are shown. Experiment was repeated using other human donors at other time points post-vaccination, as shown in Figure 2.

Dashed lines represent the limit of detection (LOD). P values are indicated. Data are represented as mean ± SEM.
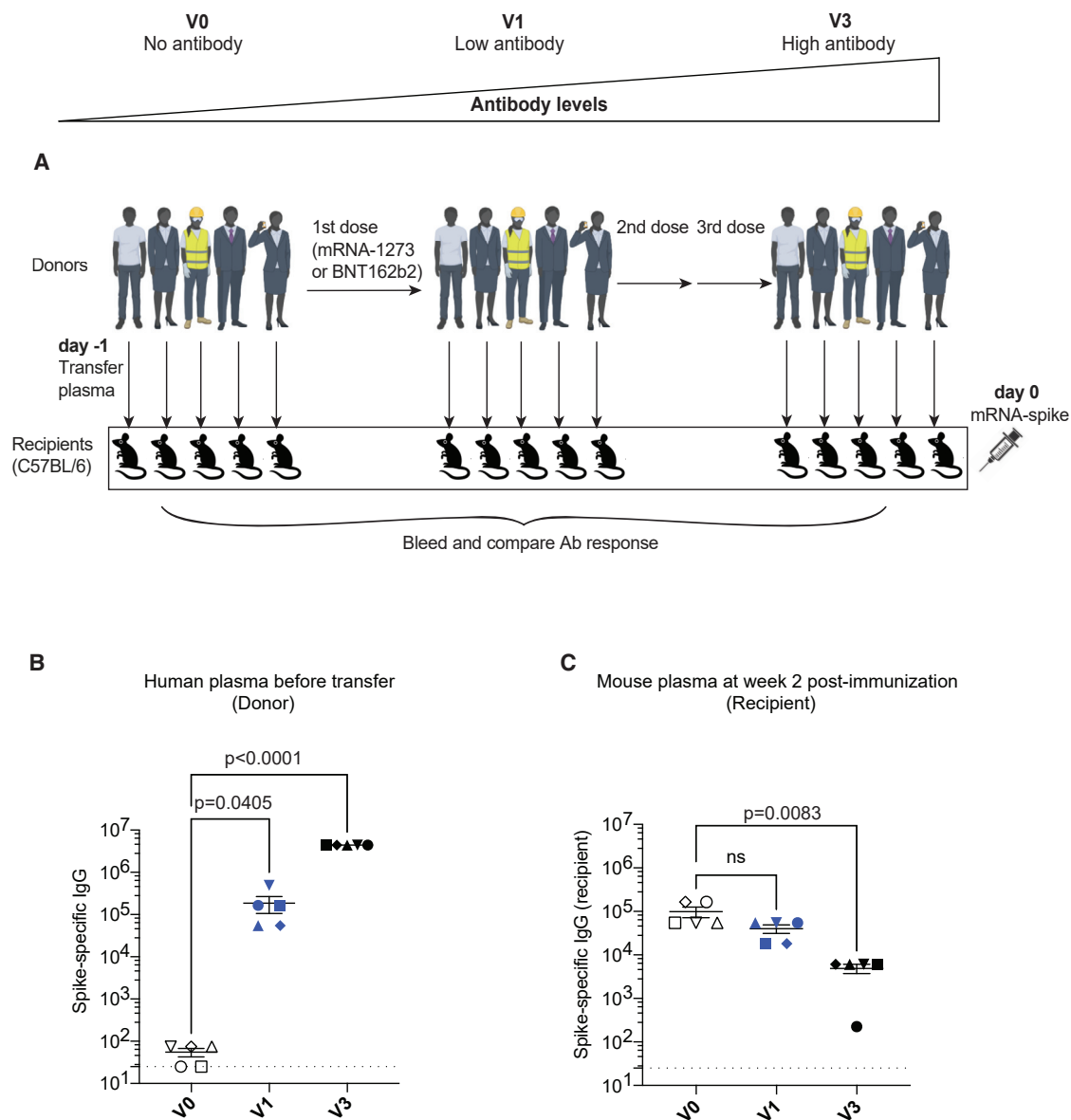
Figure 2. Inverse association between antibody titers and *de novo* antibody responses following mRNA vaccination
(A) Experimental layout. Donor-matched plasmas were harvested from five different human donors; pre-vaccination (V0), after one shot (V1 corresponding to 2–3 weeks after first dose), or after three shots (V3 corresponding to 2–3 weeks after third dose), 100 μL of these donor-matched human plasmas was adoptively transferred via the intraperitoneal route into C57BL/6 mice. On the following day, all mice were immunized intramuscularly with 3 μg of an mRNA expressing SARS-CoV-2 spike, and immune responses were quantified at week 2.
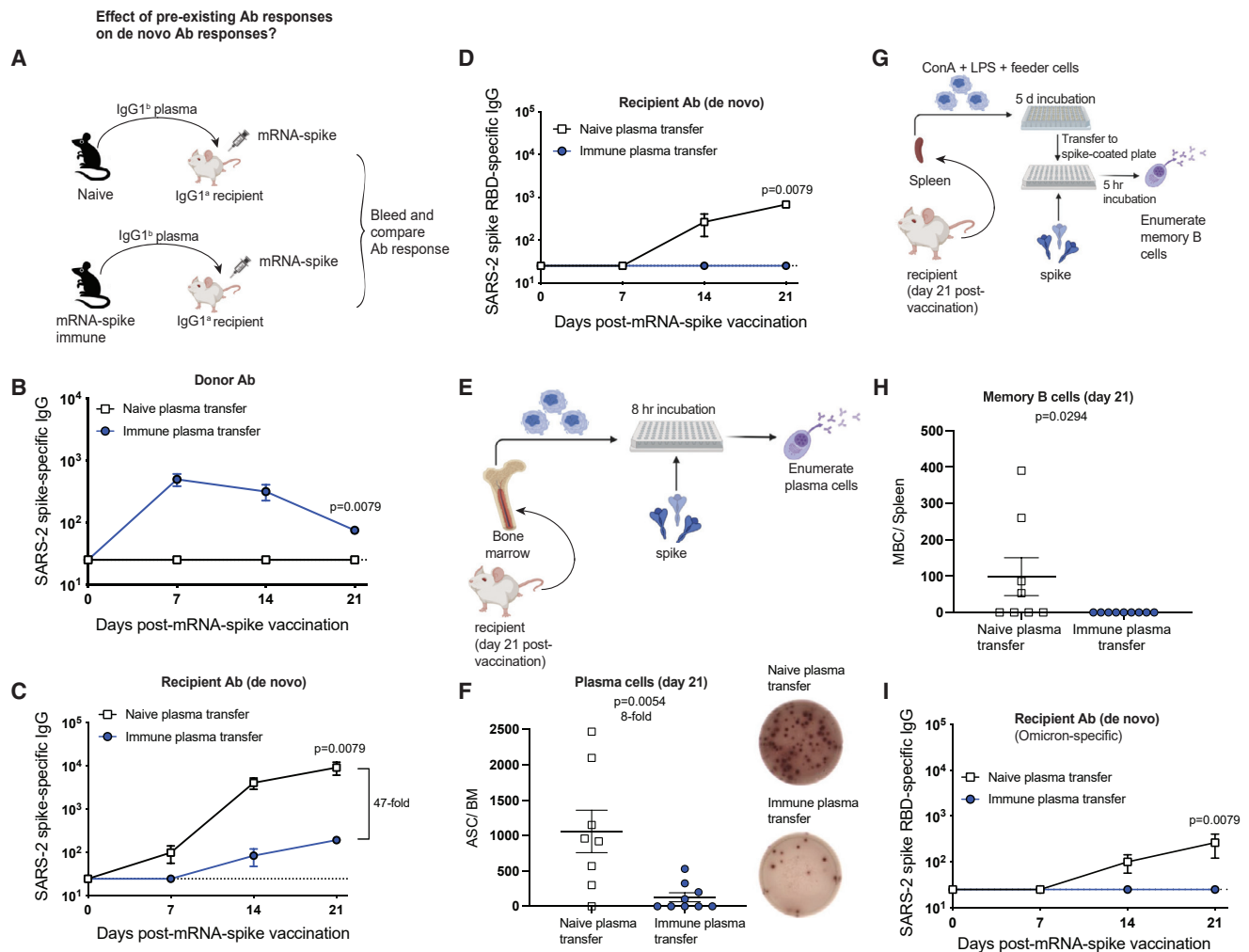(B) SARS-CoV-2 spike-specific antibody in human donors.
(C) *De novo* SARS-CoV-2 spike-specific antibody in recipient mice. Two-way ANOVA test (Dunnett's multiple comparisons, with adjusted p value) was used. p values are indicated. Data are from an experiment with five mice that received pre-vaccine human plasma (V0), five mice that received low titer human plasma (V1), and five mice that received high titer human plasma (V3); data from all experiments are shown.
Dashed lines represent the LOD. p values are indicated. Data are represented as mean ± SEM.

To bring more clarity to this issue, we primed mice with an ancestral vaccine, and then we boosted them with an ancestral or an Omicron BA.1 vaccine (Figure 4A). These vaccines were monovalent. Boosting with the ancestral vaccine generated an expected improvement in antibody responses against the ancestral virus (Figure 4B), but boosting with the Omicron vaccine did not generate superior antibody responses against Omicron (Figure 4C). Neutralizing antibody responses against the ancestral virus were 1,531-fold higher in mice that received the ancestral vaccine boost, relative to the Omicron vaccine boost (Figure 4D). Neutralizing antibody responses against Omicron were near the limit of detection in all mice but tended to be slightly higher

Figure 3. Plasma from vaccinated mice abrogates *de novo* antibody responses

(A) Experimental layout. Plasmas were harvested from C57BL/6 mice that were vaccinated with mRNA-spike (two doses). A total of 400 μL of these plasmas was adoptively transferred via the intraperitoneal route into recipient BALB/c mice. On the following day, all mice were immunized intramuscularly with 3 μg of an mRNA expressing SARS-CoV-2 spike, and immune responses were quantified longitudinally. Naive plasmas were used as control.

(B) Donor-derived SARS-CoV-2 spike-specific antibody in recipient plasma.

(C and D) Recipient-derived SARS-CoV-2 spike-specific antibody: whole spike-specific (C) and RBD-specific (D).

(E) Experimental layout for detection of antibody-secreting cells.

(F) Antibody-secreting cells in bone marrow after day 21. A representative ELISPOT well is shown to the right.

(G) Experimental layout for detection of memory B cells.

(H) Memory B cells in spleen after day 21.

(I) Recipient-derived SARS-CoV-2 Omicron RBD-specific antibody. Two-tailed Mann-Whitney test was used.

Data are from two experiments, each with three to five mice per group; the experiment was repeated for a total of two times, and all data are shown; dashed lines represent the LOD. p values are indicated. Data are represented as mean ± SEM. See also Figure S2.

(1.4-fold greater) in mice boosted with the Omicron vaccine (Figure 4E). Overall, in a host that has already been primed with an ancestral vaccine, a second shot with an Omicron vaccine did not substantially favor Omicron-specific responses, relative to a second shot with an ancestral vaccine.

We also performed homologous prime-boost regimens comparing ancestral vaccines with Omicron BA.1 vaccines (Figure 4F). Two shots of ancestral vaccine generated higher ancestral-specific antibody responses, which was expected given that the vaccine was matched to the antigen (Figure 4G). Omicron-

specific antibody responses were not significantly different after homologous prime boost (Figure 4H), but neutralizing antibody responses were higher with each "matched vaccine" (Figures 4I and 4J). In other words, although the Omicron prime-boost vaccine did not elicit superior antibody responses in terms of total binding titers (Figure 4H), it tended to elicit superior neutralizing antibodies to Omicron (Figure 4J). We did not observe differences in the number CD8 and CD4 T cells (Figures S3A–S3F), but the ancestral vaccine tended to generate slightly more polyfunctional CD8 T cell responses than the Omicron vaccine (Figures S3G and S3H).
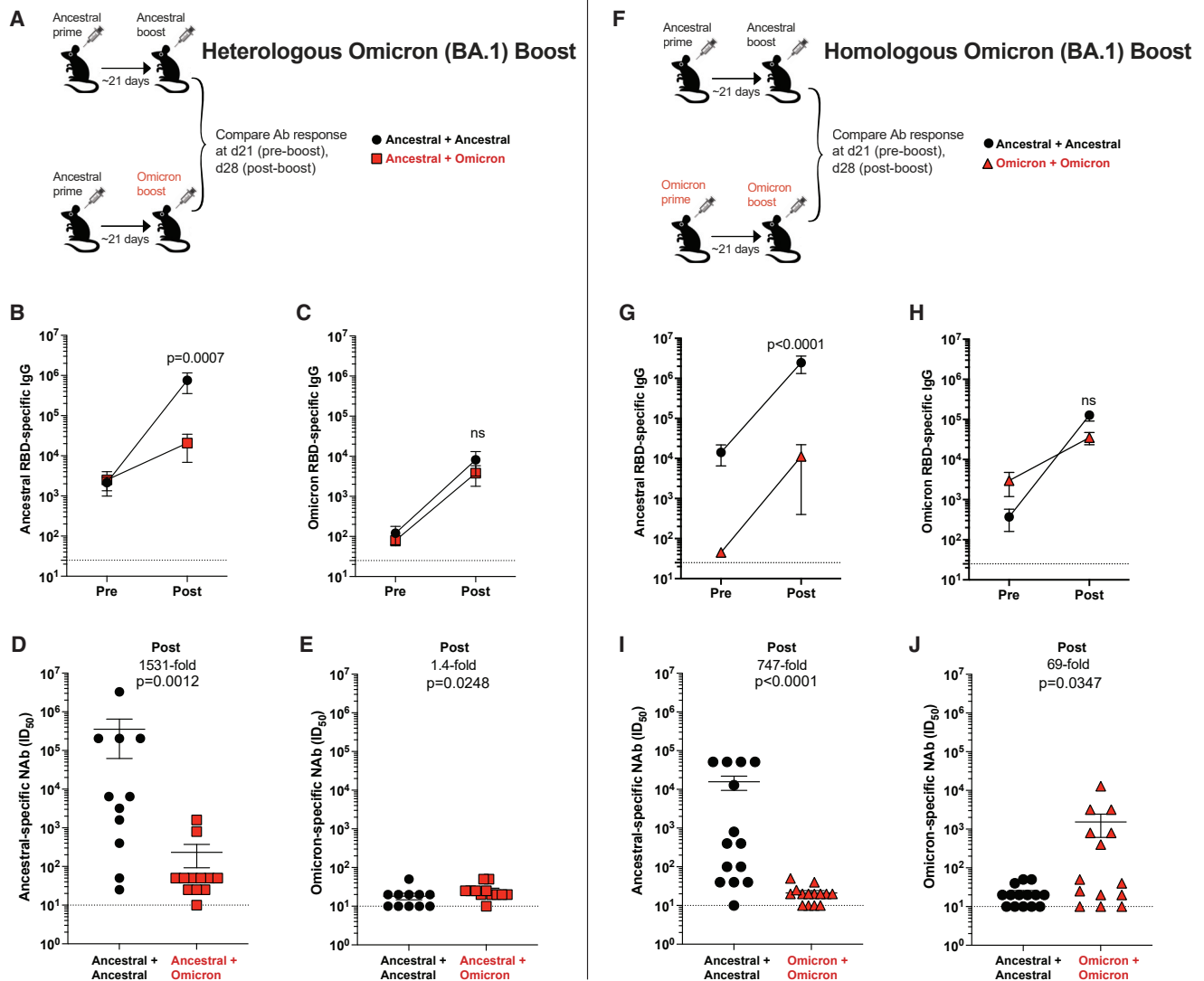
Figure 4. Comparative analyses of monovalent Omicron vaccine boosters

(A) Experimental layout for evaluating a heterologous Omicron vaccine boost. C57BL/6 mice were immunized intramuscularly with 3 μg of an mRNA expressing ancestral spike. After 3 weeks, mice were boosted with an mRNA vaccine expressing ancestral spike or Omicron spike, and immune responses were quantified.

(B) Ancestral RBD-specific antibody responses.

(C) Omicron RBD-specific antibody responses.

(D) Neutralizing antibody responses against ancestral pseudovirus.

(E) Neutralizing antibody responses against Omicron pseudovirus.

(F) Experimental layout for evaluating a homologous Omicron vaccine boost. C57BL/6 mice were immunized intramuscularly with 3 μg of an mRNA expressing ancestral spike or Omicron spike. After 3 weeks, mice were boosted homologously, and immune responses were quantified.

(G) Ancestral RBD-specific antibody responses.

(H) Omicron RBD-specific antibody responses.

(I) Neutralizing antibody responses against ancestral pseudovirus.

(J) Neutralizing antibody responses against Omicron pseudovirus. Two-tailed Mann-Whitney test was used, comparing immune responses post-boost.

Data are from three experiments with three to five mice per group; dashed lines represent the LOD. p values are indicated. Data are represented as mean ± SEM.
See also Figures S3 and S4.

To understand how each vaccine affected long-term humoral responses, we quantified plasma cells. The ancestral prime-boost regimen elicited higher numbers of ancestral-specific plasma cells and a similar number of Omicron-specific plasma cells, relative to the Omicron prime-boost regimen (Figures S3I and S3J). In addition, we compared spike protein expression on 293T cells incubated with ancestral or Omicron mRNA-LNPs, or 293T cells transfected with the respective DNA vectors used for *in vitro* transcription. The ancestral spike was expressed at higher levels relative to the Omicron spike (Figure S3K).
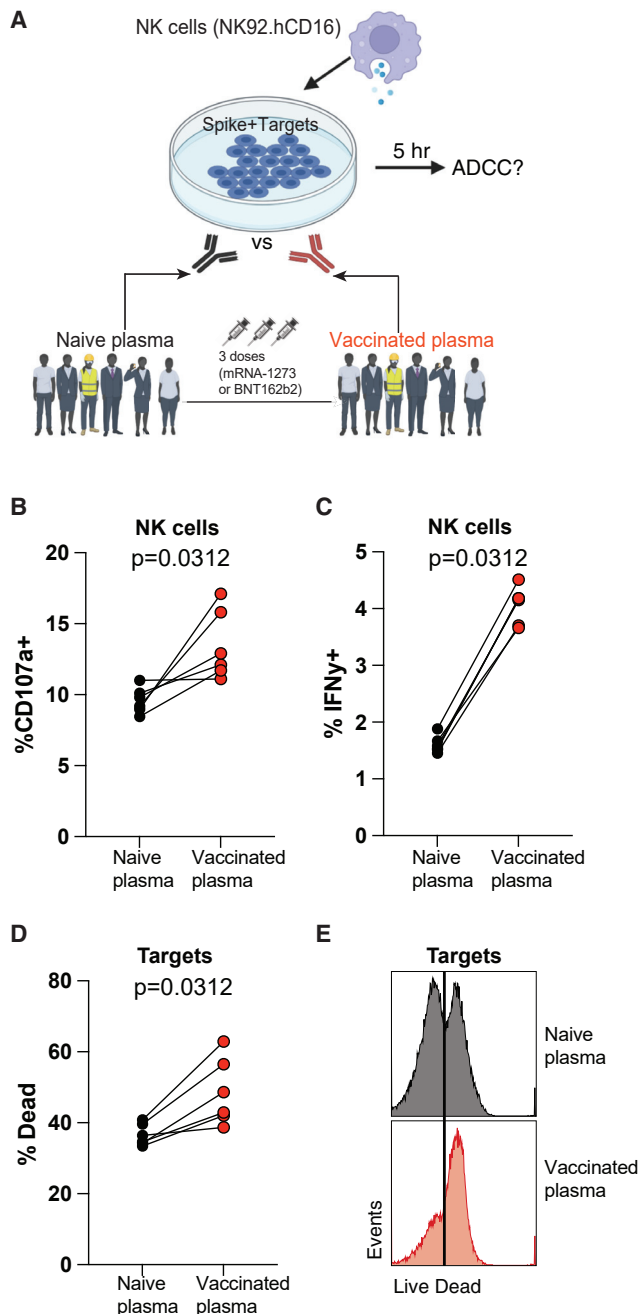
Figure 5. Vaccine-elicited plasma in humans mediates ADCC activity against target cells expressing vaccine antigen

(A) Experimental layout for evaluating ADCC activity by vaccine-elicited antibodies. 293T cells were transfected with the same DNA vector used for synthesizing the mRNA-spike vaccine. These targets were co-cultured with NK92.hCD16 effector cells and a 1:20 plasma dilution for 5 h (see STAR Methods for additional information).
(B) CD107a expression by NK92 cells.
(C) IFNγ expression by NK92 cells.
(D) Dead target cells.
(E) Representative FACS histograms showing dead target cells. Wilcoxon matched-pairs signed rank test was used. p values are indicated.
Data are from one experiment with six humans (donor-matched, pre- and post-vaccination); the experiment was performed a total of two times with similar results. See also Figures S5 and S6.

We then interrogated whether our monovalent Omicron vaccine confers superior protection to our monovalent ancestral vaccine in the setting of a single prime immunization (Figure S4A). Antibody responses tended to be higher when the vaccine antigen was matched to its respective viral antigen (Figures S4B and S4C), and this effect was also observed for neutralizing antibody responses (Figures S4D and S4E). In particular, the Omicron vaccine prime elicited 19.6-fold improved neutralizing antibody responses against Omicron (Figure S4E), and based on these data, we hypothesized that in the context of a single prime immunization, an Omicron vaccine may confer improved protection against an Omicron challenge, relative to an ancestral vaccine. To test this hypothesis, we primed K18-hACE2 mice with an ancestral vaccine or an Omicron vaccine, and at week 2 post-prime, these mice were challenged intranasally with 5×10^4 plaque-forming units (PFUs) of SARS-CoV-2 Omicron variant. Consistent with our hypothesis, we observed superior protection against Omicron in mice that received a single shot of the Omicron vaccine, relative to mice that received a single shot of the ancestral vaccine (Figure S4F). Taken together, the relative superiority of an Omicron vaccine over an ancestral vaccine may depend on whether the host has pre-existing immunity to the spike antigen.

Pre-existing immunity to the vaccine antigen limits *in situ* antigen expression after mRNA vaccination

We have demonstrated that pre-existing humoral responses abrogate *de novo* B cell responses, so next we aimed to understand a possible mechanism. Historically, the high seroprevalence of viral vectors in the human population has hampered their clinical utility both as vaccines and gene delivery systems. Pre-existing neutralizing antibodies are a main limitation for the Ad5 vector platform, because Ad5 has infected ~90% of humans, motivating the development of other vector platforms with lower seroprevalence, such as Ad26.[6–11] We interrogated whether neutralizing antibodies (which are known to limit the utility of Ad5) would also hamper the use of mRNA vaccines. Neutralizing monoclonal antibodies (mAbs) such as bamlanivimab are used for the treatment of COVID-19 in individuals at high risk for severe disease, but it is unclear whether these therapies could thwart the efficacy of mRNA vaccines. We first treated mice with a cocktail of neutralizing mAbs targeting different epitopes on the spike protein, and on the following day, we immunized these mice with the mRNA-spike vaccine (Figure S5A). The neutralizing mAbs were detectable in the circulation for more than a month (Figure S5B), but they did not significantly affect vaccine-elicited antibody responses (Figure S5C). These data suggested that the downmodulation of vaccine-elicited responses by pre-existing antibody was independent of antibody-neutralizing function.

To clarify the mechanism by which antibodies affected mRNA vaccine-elicited immunity, we performed antibody-dependent cellular cytotoxicity (ADCC) assays (Figure 5A). We co-cultured target cells expressing vaccine antigen (spike + targets) with effector NK cells and plasma from human volunteers before or after SARS-CoV-2 vaccination. After 5 h, we measured NK cytotoxic activity and target cell killing (see STAR Methods). Vaccinated plasma elicited more potent CD107a degranulation and

interferon γ (IFNγ) expression on NK cells (Figures 5B and 5C). Consistent with the increased ADCC activity triggered by vaccinated plasma, there was improved killing of target cells expressing vaccine antigen (Figures 5D and 5E). A similar increase in NK-mediated ADCC activity was observed using plasma from vaccinated mice (Figure S6). These data suggested that following a booster vaccination, cells expressing vaccine antigen can be killed by vaccine-elicited antibodies via NK-mediated effector functions.

We then asked whether pre-existing immunity to the antigen encoded by the mRNA vaccine can limit the amount of antigen that is present at the site of mRNA vaccination. To answer this simple question, we utilized an mRNA-LNP luciferase reporter that allowed *in situ* quantification of antigen expression at the site of immunization (the quadriceps muscle) in the presence or absence of pre-existing immunity. We first injected mice with this mRNA-luciferase, and after 2 weeks, we re-injected these mice with the same mRNA-luciferase to determine whether antigen clearance was accelerated during the booster immunization (Figure S7A). As controls, we injected another group of littermate control mice with PBS, and after 2 weeks, we injected these mice with mRNA-luciferase. Interestingly, mice that received the mRNA-LNP for the second time showed significantly lower antigen levels by *in vivo* luminescence imaging (IVIS), relative to mice that received the mRNA-LNP for the first time (Figures S7B and S7C). These data suggest that pre-existing immunity limits the amount of antigen available after mRNA-LNP re-utilization.

To evaluate a more specific role for humoral immunity, we performed a passive immunization study using plasma from immune mice (Figure 6A). We primed C57BL/6 mice with mRNA-luciferase, and after 3 weeks, we boosted these same mice with the same mRNA-luciferase to generate a high level of luciferase-specific antibodies (Figure S7D). These mice were bled, and immune plasma was adoptively transferred into naive BALB/c mice. As controls, we transferred plasma from mice that were previously immunized with a control mRNA-LNP expressing an irrelevant antigen (mRNA-spike). A day after adoptive plasma transfer, all mice received an intramuscular injection of mRNA-luciferase, and the kinetics of antigen clearance was quantified by IVIS. Injection of mRNA-luciferase into recipient mice resulted in rapid antigen expression by 6 h post-immunization, and most of the antigen was cleared after 1 day of immunization (Figures 6B and 6C). Interestingly, transfer of luciferase-specific plasma accelerated antigen clearance after mRNA immunization, demonstrating that seropositivity to the antigen encoded by the mRNA vaccine limits the amount of antigen at the site of immunization (Figures 6B and 6C). We also evaluated whether humoral responses elicited by a different vaccine platform could have a similar effect on antigen clearance. To test this, we included mice that received a different vaccine platform expressing the same antigen (Ad5-luciferase) (Figure 6D). Humoral responses elicited by an Ad5-luciferase vector also accelerated antigen clearance following mRNA-luciferase vaccination (Figures 6E and 6F). These data suggested that humoral responses against the transgene itself (luciferase) could accelerate antigen clearance following mRNA vaccination.

Finally, we asked whether the clearance of vaccine antigen by pre-existing antibody responses was dependent on antibody effector mechanisms. To answer this question, we purified IgG from the plasma of mRNA-luciferase-immunized mice, followed by digestion with pepsin, which cleaves IgG into an F(ab′)2 fragment and an Fc fragment. We then transferred this F(ab′)2 fragment into naive mice, followed by immunization with mRNA-luciferase 1 day later (Figure S7E). Note that the F(ab′)2 fragment retains antigen-binding capacity but is devoid of effector function because of the absence of the Fc fragment (Figures S7F and S7G). Importantly, the F(ab′)2 fragment from immune IgG did not accelerate antigen clearance after mRNA immunization, suggesting that antibody effector mechanisms were required for the clearance of vaccine antigen (Figures S7H and S7I). Luciferase is known to be an intracellular protein, but we asked whether this protein can be present and thus recognized by luciferase-specific antibodies at the surface of the cell. To examine this, we performed surface staining of luciferase+ 293T cells with luciferase-specific immune plasma, followed by staining with a fluorescently labeled anti-mouse IgG. Most luciferase binding was observed after intracellular staining, consistent with the intracellular localization of this reporter protein, but surface binding was also observed, albeit at lower levels (Figures S7J and S7K). This result was consistent with prior studies showing that proteins that are normally present intracellularly can also be presented at the surface of the cell and be recognized by antibodies with effector function.[12–14] In addition, we evaluated whether the Fc fragment of pre-existing antibodies was required for downmodulation of *de novo* antibody responses. To determine this, we purified IgG from the plasma of mRNA-spike-immunized mice, followed by digestion with pepsin, to generate an F(ab′)2 fragment devoid of effector function. We then transferred this F(ab′)2 fragment into naive mice, followed by immunization with mRNA-spike 1 day later (Figure S7L). The F(ab′)2 fragment from immune IgG did not significantly affect *de novo* antibody responses after mRNA immunization (Figure S7M). Taken together, we show that pre-existing antibody elicited by prior immunization accelerates antigen clearance following mRNA vaccination, via an Fc-dependent effector mechanism that significantly limits the amount of antigen available to prime B cell responses.

Generalizability to an mRNA-HIV vaccine
So far, we have demonstrated that pre-existing SARS-CoV-2 spike-specific antibody responses limit antibody responses generated by mRNA-based SARS-CoV-2 vaccines. Due to their extraordinary success during the COVID-19 pandemic, mRNA vaccines are now being explored for multiple diseases, and there are several ongoing HIV vaccine trials using the mRNA vaccine platform (ClinicalTrials.gov: NCT05217641). Thus, we interrogated the effects of pre-existing humoral responses on an mRNA-based HIV vaccine. We developed an mRNA vaccine expressing a clade B envelope derived from HIV-1 strain SF162 (mRNA-HIV), and we immunized C57BL/6 mice with this mRNA-HIV vaccine or a control ancestral SARS-CoV-2 vaccine (mRNA-spike). We boosted mice after 4 weeks to generate a high titer of virus-specific antibodies, and at week 2 post-boost, we harvested immune plasma and transferred it to naive BALB/c recipient mice. On the following day, we immunized recipient mice with the mRNA-HIV vaccine
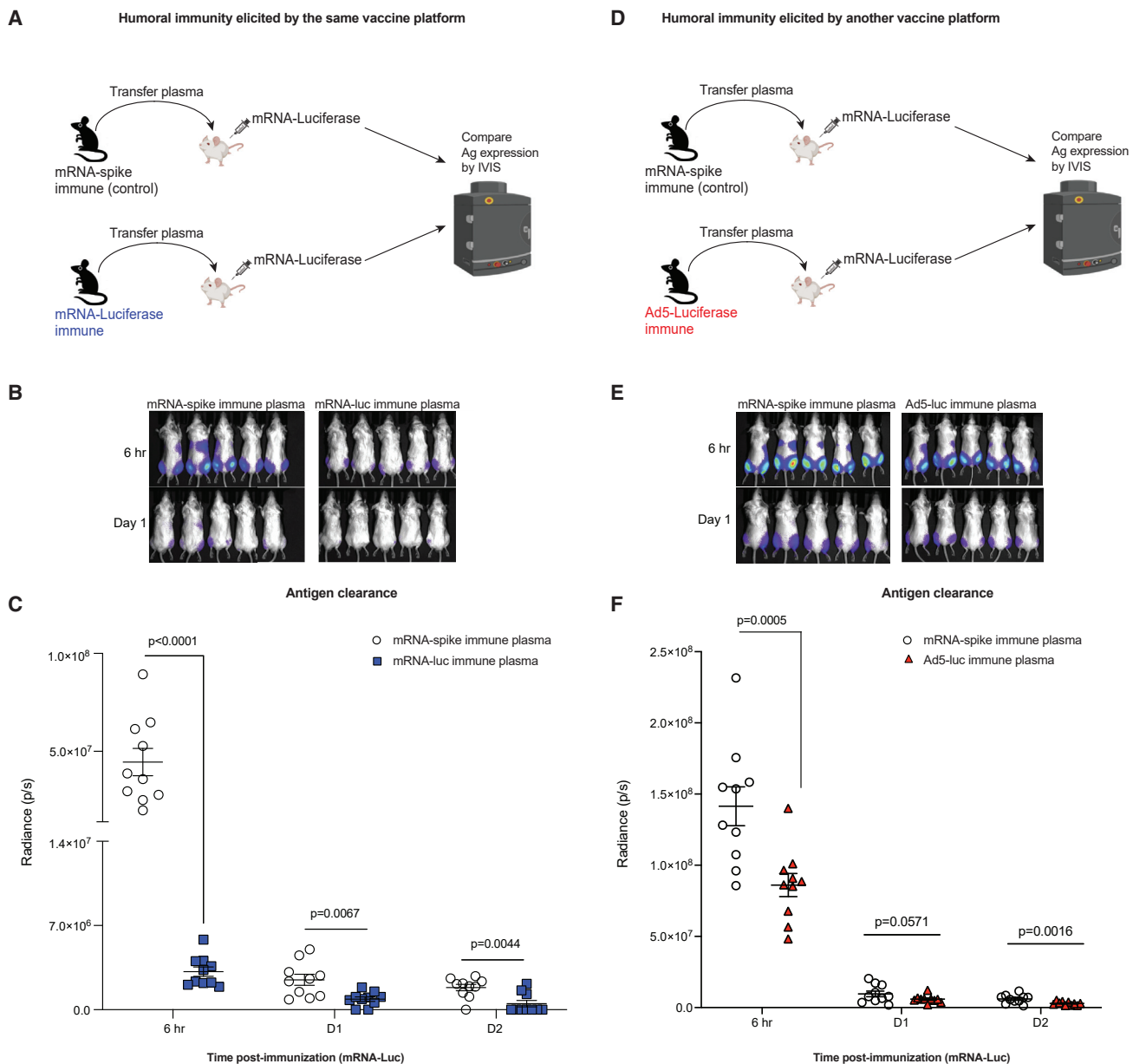
Figure 6. Humoral responses limit antigen levels following mRNA immunization

(A) Experimental layout for evaluating the effect of humoral responses on antigen clearance. C57BL/6 mice were immunized intramuscularly with 3 µg of an mRNA expressing a luciferase reporter and after 3 weeks, mice were boosted. We immunized another group of mice with an irrelevant mRNA vaccine expressing a different antigen (mRNA-spike). Two weeks after boost, mice were bled, and plasmas were collected. A total of 400 µL of these plasmas was adoptively transferred into naive BALB/c mice via the intraperitoneal route. On the following day, recipient mice received an intramuscular injection of mRNA-luciferase, and luciferase expression was quantified by *in vivo* imaging (IVIS).

(B) Bioluminescence images.

(C) Summary of antigen expression by IVIS.

(D) Experimental layout for evaluating the effect of antigen-specific humoral responses on antigen clearance. Experiment was similar to that of (A), but we immunized another group of mice with a different vaccine platform expressing the same transgene (Ad5-luciferase).

(E) Bioluminescence images.

(F) Summary of antigen expression by IVIS.

Data are from one experiment with 10 quadriceps per group (five mice per group). Experiment was repeated for a total of three times, with similar results. Two-tailed Mann-Whitney test was used. p values are indicated. Data are represented as mean ± SEM. See also Figure S7.

A   Effect of pre-existing HIV-specific responses
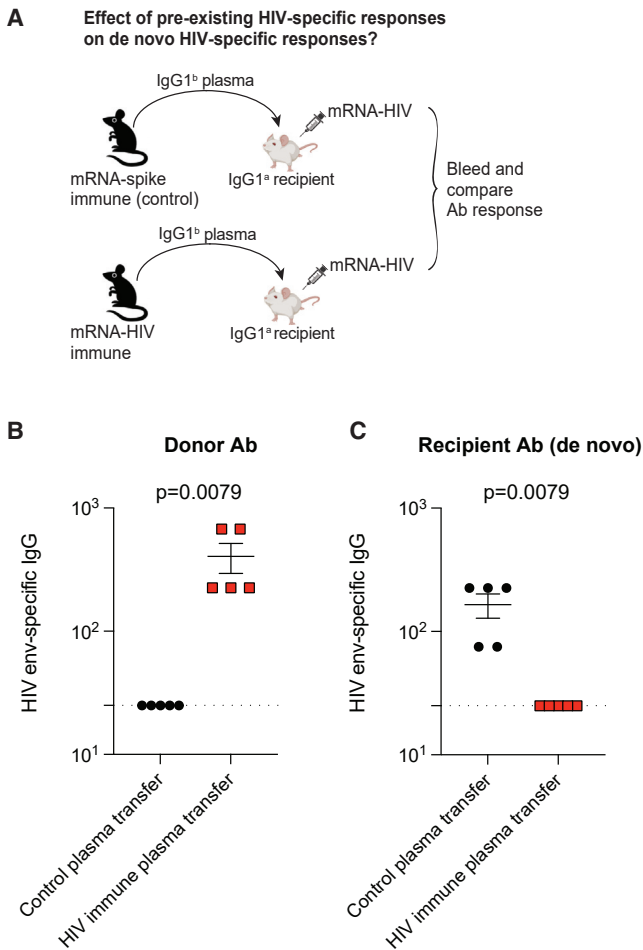on de novo HIV-specific responses?

Figure 7. Pre-existing humoral responses limit the immunogenicity of an mRNA-HIV vaccine

(A) Experimental layout. Plasmas were harvested from C57BL/6 mice that were vaccinated with a control vaccine (mRNA-spike) or an HIV vaccine (mRNA-HIV) (two doses). A total of 400 μL of these plasmas was adoptively transferred via the intraperitoneal route into recipient BALB/c mice. On the following day, all mice were immunized intramuscularly with 5 μg of an mRNA expressing HIV-1 SF162 envelope, and immune responses were quantified after 2 weeks.

(B) Donor-derived HIV envelope-specific antibody in recipient plasma.

(C) Recipient-derived HIV envelope-specific antibody in recipient plasma. Two-tailed Mann-Whitney test was used.

Data are from one experiment, each with five mice per group. All data are shown; dashed lines represent the LOD. p values are indicated. Data are represented as mean ± SEM.

and compared antibody responses (Figure 7A). Similar to our prior experiments, antibodies from donor mice and recipient mice were distinguished based on their IgG1 allotype. We were able to detect donor antibodies in mice that received HIV-specific plasma (Figure 7B) and, consistent with our prior data, we also observed a negative effect of pre-existing HIV-specific antibodies on mRNA-HIV vaccines (Figure 7C), demonstrating that the findings were generalizable to other mRNA vaccines. Overall, we show that pre-existing antibodies can limit *de novo* antibody responses elicited by mRNA vaccines.

DISCUSSION

mRNA vaccines have been administered to millions of people worldwide and have shown high efficacy at preventing COVID-19. Despite their success, breakthrough infections, variants of concern, and declining antibody levels have warranted the use of boosters. It remains unclear how pre-existing immunity induced by prior vaccinations or infections affects the efficacy of mRNA vaccines. By analyzing a cohort of individuals who were initially primed with mRNA vaccines, we observed that lower antibody levels before the boost were associated with higher fold-increase in antibody levels after the boost. We show the same inverse correlation in COVID-19 convalescent patients who subsequently received SARS-CoV-2 vaccines. Similar results have been shown by other groups,[15–17] but the mechanism has been unclear.

To further examine the effects of pre-existing immunity on mRNA vaccines, we performed passive immunization studies in mice, transferring plasma from vaccinated humans into mice that were later immunized with mRNA vaccines. Transfer of immune plasma into recipient mice abrogated *de novo* priming of B cell responses following mRNA-spike vaccination. Similar effects were reported in mice that received autologous (mouse-derived) immune plasma. At first glance, these data supported a model in which systemic antibodies "compete" with B cells, arguing in favor of extending prime-boost intervals to allow systemic antibody levels to decline. It has been shown that extended prime-boost intervals elicit more potent antibody responses,[11,18] but it has been unclear whether this effect is due to a time-dependent maturation of immune responses, competition between antibodies and B cells for antigen, or another mechanism. During a secondary antigen encounter, there can be competition between primary and secondary T cell responses, as well as primary and secondary B cell responses.[3,11,19] Our initial hypothesis was simply that on a booster immunization, antibodies elicited by a previous immunization "competed" with B cells by masking the antigen. Consistent with this hypothesis, we observed a pattern of reduced responses after immune F(ab')2 transfer compared with naive IgG transfer (Figure S7M), although the difference was not statistically significant. Our experiments using F(ab')2 fragments (which retain antigen binding without effector function) suggest that in addition to antigen masking, antibody effector functions could also be mechanistically involved. It is important to highlight that F(ab')2 exhibits less stability relative to intact antibody,[20,21] but our analyses comparing antigen clearance are at hyperacute time points (6 h; Figures S7H and S7I).

Our data do not suggest that booster immunizations do not work. The mRNA boosting still conferred an immunological benefit because it increased antibody titers, but the data suggested that as antibody responses reach a certain level, it becomes increasingly harder to improve responses. In addition, our data suggest that convalescent plasma therapy can hamper the efficacy of mRNA vaccines. Plasma contains antibodies with various types of function, such as neutralizing and effector functions. We did not observe a significant effect of neutralizing mAbs on mRNA vaccine-elicited responses, consistent with prior reports.[22,23] This could be explained by the antibody

isotypes and the functions that they trigger. The neutralizing mAbs used in our study were IgG1, and this isotype is typically not a potent inducer for ADCC activity in mice.[24] However, immune plasma contains many isotypes, such as IgG2a and IgG2b, which are known to mediate potent ADCC activity in mice.[24] Importantly, the cocktail of neutralizing mAbs used in our study binds to two distinct epitopes on the spike protein, so the data in Figure S5 suggest that competition for antigen may not be as critical as antibody effector mechanisms at curtailing *de novo* antibody responses after vaccination. The findings in the present study may also help guide the optimal time for vaccinating, ideally after plasma ADCC activity has contracted or after convalescent plasma has been cleared from circulation.

We also evaluated whether pre-existing antibody affected the kinetics of antigen clearance following mRNA vaccination. We quantified vaccine antigen using an mRNA-LNP expressing a luciferase reporter, which allowed sensitive quantification of antigen levels in the presence or absence of pre-existing immunity. Our data showed that pre-existing immunity against the transgene itself accelerates antigen clearance after mRNA immunization. In the case of adenovirus vaccines, pre-existing neutralizing antibodies elicited by prior immunizations are thought to block the entry of these vectors into host cells, limiting their clinical utility and motivating the use of adenoviruses with lower seroprevalence, such as Ad26. However, mRNA vaccines may be unaffected by neutralizing antibodies, especially because the antigen is expressed only after the mRNA enters the host cell.

It is unclear why T cell responses were not affected by pre-existing antibody responses. A prior clinical study in volunteers who received dose-escalating doses of the Pfizer vaccine (BNT162b1) showed that antibody responses were higher with greater mRNA vaccine doses, whereas T cell responses were not higher with greater vaccine doses.[25] Prior studies have suggested that T cells may require less antigen to undergo expansion relative to B cells,[26–28] and it is possible that after a certain "antigen threshold," more antigen may not necessarily result in more T cell expansion. Another question from our studies is why T cell responses were similar following ancestral vaccination or Omicron vaccination, whereas antibody responses differed. This may be because of the way that T cells and B cells recognize their cognate antigen. B cells recognize three-dimensional structures on the antigen, whereas T cells recognize short linear epitopes, so T cells may not be substantially affected by structural features of the Omicron spike protein.[29–31]

Pre-existing humoral immunity extends beyond what is conferred by plasma transfer, and it would be interesting to examine how pre-existing antibody responses interact with MBCs and ongoing germinal center (GC) reactions, which can persist for months.[32–34] It is possible that following a secondary immunization, antibodies can also accelerate the clearance of antigen within the GC, which could potentially affect the evolution of GC B cells, but more studies are needed to understand the interplay between circulating antibody responses and ongoing GC B cell responses. Due to the growing interest in updated booster vaccines, we also investigated how pre-existing immunity affects the immunogenicity of booster vaccines based on the Omicron variant. Our data show that boosting a seropos-

itive host with a monovalent Omicron BA.1 vaccine may not confer a substantial immunological advantage, relative to boosting with an ancestral vaccine. In this regard, original antigenic sin has been suggested to affect the elicitation of Omicron-specific immune responses in a host that has been previously immunized with ancestral antigen.[35,36] The "vaccine antigen clearance" effect by pre-existing antibodies reported in our study may also help explain the factors that influence original antigen sin, an incompletely understood phenomenon that was first identified by Thomas Francis in the 1960s to describe how responses to an initial influenza infection affect responses to subsequent influenza infections.[37]

There are differences between our Omicron vaccine and the recently deployed Pfizer-BioNTech and Moderna Omicron vaccines. First, our Omicron vaccine is monovalent, whereas the recently deployed Omicron vaccines are bivalent. Second, our Omicron vaccine was administered as a second shot, whereas the recently deployed Omicron vaccines are being administered mostly as a fourth shot. Third, our Omicron vaccine is based only on BA.1, whereas the recently deployed Omicron vaccines are based on later variants. Despite these differences, there are similarities between our study and the studies with the recently deployed vaccines. For example, the Moderna bivalent booster elicited a 1.7× enhancement in neutralizing antibodies (NAb) against Omicron, relative to ancestral booster. Our data in Figure 4E show a similar trend: 1.4× enhancement in NAb against Omicron, relative to ancestral booster. Ultimately, our data do not contradict the clinical studies with the updated Omicron vaccines. On the contrary, our data suggest that the decision of implementing a bivalent vaccine is reasonable, given the limitations that we report for a monovalent BA.1 Omicron vaccine.

Furthermore, we show that in the context of a single prime, an Omicron vaccine may confer a slight but statistically significant protective advantage against Omicron, relative to an ancestral vaccine. This advantage is mostly lost in a seropositive host, suggesting that the relative superiority of an Omicron vaccine depends on whether the host is immune to SARS-CoV-2. These results can help guide the appropriate deployment of updated vaccines to relevant human populations. For instance, in a naive or seronegative population with high risk for Omicron infection, an Omicron primary vaccine may confer a slight protective advantage compared with an ancestral primary vaccine. However, this relative benefit of immunizing with an Omicron vaccine may be less striking in a population with pre-existing immunity to the ancestral virus. We also evaluated immune responses after homologous prime-boost immunizations, comparing an ancestral vaccine with an Omicron vaccine. Priming and boosting with the same ancestral vaccine elicited substantially higher levels of ancestral-specific antibody responses, relative to priming and boosting with the Omicron vaccine. This is an expected outcome because the vaccine antigen is matched. However, an unexpected finding is that priming and boosting with the monovalent Omicron vaccine did not elicit substantially higher levels of Omicron-specific responses. Such effect could be because of the structural stability of the Omicron spike protein, which has been suggested to be a poor immunogen.[29–31] Our side-by-side comparison of antigen expression on 293T cells revealed lower levels of translated spike protein with the monovalent

Omicron BA.1 vaccine relative to the ancestral vaccine, which may advise in favor of bivalent vaccines, including spike sequences other than that of BA.1. Because variant-specific vaccines are being developed around the globe, it is important to consider not only "antigenic matching" of the vaccine antigen to circulating variants but also the structural stability of the vaccine antigen, because both can affect the immunogenicity of vaccines. The development of SARS-CoV-2 vaccines was in part possible by introducing stabilizing amino acids in the ancestral spike protein (two prolines at position 986–987), suggesting that structural stability can be crucially important in vaccines.[38,39]

In summary, there are two critical points from this study. First, pre-existing antibody limits *de novo* B cell responses following mRNA vaccination. This observation agrees with the recommendation of increasing prime-boost intervals, to allow systemic antibody levels to decline. Similarly, in the context of convalescent plasma therapy, it may be beneficial to wait until passively transferred antibodies are cleared from circulation before administering mRNA vaccines. We did not observe impairment of vaccine-elicited responses by neutralizing mAb therapy, but our data suggest that treatment with antibodies that trigger ADCC activity (which are being developed for HIV[40–42]) may have detrimental effects if administered during mRNA vaccination. Second, pre-existing antibody to the antigen encoded by the mRNA vaccine accelerates the clearance of the antigen at the site of immunization via antibody effector mechanisms, severely limiting the amount of antigen available to prime B cell responses. Future studies will determine whether experimental blockade of ADCC activity during mRNA booster immunization can delay the clearance of vaccine antigen and enhance vaccine-elicited responses. Finally, there are several trials testing mRNA vaccines against multiple infectious diseases, and our data with mRNA-HIV vaccines suggest generalizability. Overall, these data are important for understanding how pre-existing immunity modulates responses to mRNA boosters, providing insights to improve this delivery platform in next-generation vaccines.

Limitations of the study

Our experiments show that NK cells trigger ADCC by plasma antibodies, but NK cells are not the only cells that mediate ADCC *in vivo*. Future studies will examine the contribution of other cell subsets, such as macrophages and neutrophils. Our studies suggest a role for ADCC, but further studies are needed to determine the contribution of other antibody effector mechanisms, including antibody-dependent cellular phagocytosis (ADCP).

STAR★METHODS

Detailed methods are provided in the online version of this paper and include the following:

- KEY RESOURCES TABLE
- RESOURCE AVAILABILITY
  - Lead contact
  - Materials availability
  - Data and code availability
- EXPERIMENTAL MODELS AND SUBJECT DETAILS
  - Animals and ethics statement

- METHOD DETAILS
  - Mice and vaccinations
  - SARS-CoV-2 virus and infections
  - SARS-CoV-2 quantification in lungs
  - Reagents, flow cytometry and equipment
  - SARS-CoV-2 spike and luciferase specific ELISA
  - ADCC assays
  - Surface binding of luciferase-specific antibodies from plasma
  - mRNA-LNP vaccines
  - *In vivo* bioluminescence
  - Pseudovirus neutralization assays
  - B cell ELISPOT
  - IgG purification from plasma and generation of F(ab')2 fragments
  - Comparing spike protein expression by ancestral and Omicron vaccines
- QUANTIFICATION AND STATISTICAL ANALYSIS

REFERENCES

1. Ying, B., Scheaffer, S.M., Whitener, B., Liang, C.Y., Dmytrenko, O., Mackin, S., Wu, K., Lee, D., Avena, L.E., Chong, Z., et al. (2022). Boosting with variant-matched or historical mRNA vaccines protects against Omicron infection in mice. Cell *185*, 1572–1587.e11. https://doi.org/10.1016/j.cell.2022.03.037.

2. Gagne, M., Moliva, J.I., Foulds, K.E., Andrew, S.F., Flynn, B.J., Werner, A.P., Wagner, D.A., Teng, I.T., Lin, B.C., Moore, C., et al. (2022). mRNA-1273 or mRNA-Omicron boost in vaccinated macaques elicits similar B cell expansion, neutralizing responses, and protection from Omicron. Cell *185*, 1556–1571.e18. https://doi.org/10.1016/j.cell.2022.03.038.

3. Mesin, L., Schiepers, A., Ersching, J., Barbulescu, A., Cavazzoni, C.B., Angelini, A., Okada, T., Kurosaki, T., and Victora, G.D. (2020). Restricted clonality and limited germinal center reentry characterize memory B cell reactivation by boosting. Cell 180, 92–106.e11. https://doi.org/10.1016/j.cell.2019.11.032.

4. Slifka, M.K., Antia, R., Whitmire, J.K., and Ahmed, R. (1998). Humoral immunity due to long-lived plasma cells. Immunity 8, 363–372. https://doi.org/10.1016/s1074-7613(00)80541-5.

5. Koutsakos, M., and Ellebedy, A.H. (2022). Long live the plasma cell: the basis of sustained humoral immunity. J. Immunol. 209, 3–4. https://doi.org/10.4049/jimmunol.2200121.

6. Barouch, D.H., Kik, S.V., Weverling, G.J., Dilan, R., King, S.L., Maxfield, L.F., Clark, S., Ng'ang'a, D., Brandariz, K.L., Abbink, P., et al. (2011). International seroepidemiology of adenovirus serotypes 5, 26, 35, and 48 in pediatric and adult populations. Vaccine 29, 5203–5209. https://doi.org/10.1016/j.vaccine.2011.05.025.

7. Penaloza-MacMaster, P., Alayo, Q.A., Ra, J., Provine, N.M., Larocca, R., Lee, B., and Barouch, D.H. (2016). Inhibitory receptor expression on memory CD8 T cells following Ad vector immunization. Vaccine 34, 4955–4963. https://doi.org/10.1016/j.vaccine.2016.08.048.

8. Penaloza-MacMaster, P., Provine, N.M., Ra, J., Borducchi, E.N., McNally, A., Simmons, N.L., Iampietro, M.J., and Barouch, D.H. (2013). Alternative serotype adenovirus vaccine vectors elicit memory T cells with enhanced anamnestic capacity compared to Ad5 vectors. J. Virol. 87, 1373–1384. https://doi.org/10.1128/JVI.02058-12.

9. Tan, W.G., Jin, H.-T., West, E.E., Penaloza-MacMaster, P., Wieland, A., Zilliox, M.J., McElrath, M.J., Barouch, D.H., and Ahmed, R. (2013). Comparative analysis of simian immunodeficiency virus gag-specific effector and memory CD8+ T cells induced by different adenovirus vectors. J. Virol. 87, 1359–1372. https://doi.org/10.1128/JVI.02055-12.

10. Buchbinder, S.P., Mehrotra, D.V., Duerr, A., Fitzgerald, D.W., Mogg, R., Li, D., Gilbert, P.B., Lama, J.R., Marmor, M., Del Rio, C., et al. (2008). Efficacy assessment of a cell-mediated immunity HIV-1 vaccine (the Step Study): a double-blind, randomised, placebo-controlled, test-of-concept trial. Lancet 372, 1881–1893. https://doi.org/10.1016/S0140-6736(08)61591-3.

11. Sanchez, S., Palacio, N., Dangi, T., Ciucci, T., and Penaloza-MacMaster, P. (2021). Fractionating a COVID-19 Ad5-vectored vaccine improves virus-specific immunity. Sci. Immunol. 6, eabi8635. https://doi.org/10.1126/sciimmunol.abi8635.

12. Dangi, T., Sanchez, S., Class, J., Richner, M., Visvabharathy, L., Chung, Y.R., Bentley, K., Stanton, R.J., Koralnik, I.J., Richner, J.M., and Penaloza-MacMaster, P. (2022). Improved control of SARS-CoV-2 by treatment with nucleocapsid-specific monoclonal antibody. J. Clin. Invest. 132, e162282. https://doi.org/10.1172/JCI162282.

13. López-Muñoz, A.D., Kosik, I., Holly, J., and Yewdell, J.W. (2022). Cell surface SARS-CoV-2 nucleocapsid protein modulates innate and adaptive immunity. Sci. Adv. 8, eabp9770. https://doi.org/10.1126/sciadv.abp9770.

14. Fielding, C.A., Sabberwal, P., Williamson, J.C., Greenwood, E.J.D., Crozier, T.W.M., Zelek, W., Seow, J., Graham, C., Huettner, I., Edgeworth, J.D., et al. (2022). SARS-CoV-2 host-shutoff impacts innate NK cell functions, but antibody-dependent NK activity is strongly activated through non-spike antibodies. Elife 11, e74489. https://doi.org/10.7554/eLife.74489.

15. Sasaki, S., He, X.S., Holmes, T.H., Dekker, C.L., Kemble, G.W., Arvin, A.M., and Greenberg, H.B. (2008). Influence of prior influenza vaccination on antibody and B-cell responses. PLoS One 3, e2975. https://doi.org/10.1371/journal.pone.0002975.

16. Gilbert, P.B., Gabriel, E.E., Miao, X., Li, X., Su, S.C., Parrino, J., and Chan, I.S.F. (2014). Fold rise in antibody titers by measured by glycoprotein-based enzyme-linked immunosorbent assay is an excellent correlate of protection for a herpes zoster vaccine, demonstrated via the vaccine efficacy curve. J. Infect. Dis. 210, 1573–1581. https://doi.org/10.1093/infdis/jiu279.

17. Goel, R.R., Apostolidis, S.A., Painter, M.M., Mathew, D., Pattekar, A., Kuthuru, O., Gouma, S., Hicks, P., Meng, W., Rosenfeld, A.M., et al. (2021). Distinct antibody and memory B cell responses in SARS-CoV-2 naive and recovered individuals following mRNA vaccination. Sci. Immunol. 6, eabi6950. https://doi.org/10.1126/sciimmunol.abi6950.

18. Goel, R.R., Painter, M.M., Lundgreen, K.A., Apostolidis, S.A., Baxter, A.E., Giles, J.R., Mathew, D., Pattekar, A., Reynaldi, A., Khoury, D.S., et al. (2022). Efficient recall of Omicron-reactive B cell memory after a third dose of SARS-CoV-2 mRNA vaccine. Cell 185, 1875–1887.e8. https://doi.org/10.1016/j.cell.2022.04.009.

19. Penaloza-MacMaster, P., Teigler, J.E., Obeng, R.C., Kang, Z.H., Provine, N.M., Parenteau, L., Blackmore, S., Ra, J., Borducchi, E.N., and Barouch, D.H. (2014). Augmented replicative capacity of the boosting antigen improves the protective efficacy of heterologous prime-boost vaccine regimens. J. Virol. 88, 6243–6254. https://doi.org/10.1128/JVI.00406-14.

20. Gadkar, K., Pastuskovas, C.V., Le Couter, J.E., Elliott, J.M., Zhang, J., Lee, C.V., Sanowar, S., Fuh, G., Kim, H.S., Lombana, T.N., et al. (2015). Design and pharmacokinetic characterization of novel antibody formats for ocular therapeutics. Invest. Ophthalmol. Vis. Sci. 56, 5390–5400. https://doi.org/10.1167/iovs.15-17108.

21. Buist, M.R., Kenemans, P., den Hollander, W., Vermorken, J.B., Molthoff, C.J., Burger, C.W., Helmerhorst, T.J., Baak, J.P., and Roos, J.C. (1993). Kinetics and tissue distribution of the radiolabeled chimeric monoclonal antibody MOv18 IgG and F(ab')2 fragments in ovarian carcinoma patients. Cancer Res. 53, 5413–5418.

22. Nkolola, J.P., Yu, J., Wan, H., Chang, A., McMahan, K., Anioke, T., Jacob-Dolan, C., Powers, O., Ye, T., Chandrashekar, A., et al. (2022). A bivalent SARS-CoV-2 monoclonal antibody combination does not affect the immunogenicity of a vector-based COVID-19 vaccine in macaques. Sci. Transl. Med. 14, eabo6160. https://doi.org/10.1126/scitranslmed.abo6160.

23. Benschop, R.J., Tuttle, J.L., Zhang, L., Poorbaugh, J., Kallewaard, N.L., Vaillancourt, P., Crisp, M., Trinh, T.N.V., Freitas, J.J., Beasley, S., et al. (2022). The anti-SARS-CoV-2 monoclonal antibody bamlanivimab minimally affects the endogenous immune response to COVID-19 vaccination. Sci. Transl. Med. 14, eabn3041. https://doi.org/10.1126/scitranslmed.abn3041.

24. Kipps, T.J., Parham, P., Punt, J., and Herzenberg, L.A. (1985). Importance of immunoglobulin isotype in human antibody-dependent, cell-mediated cytotoxicity directed by murine monoclonal antibodies. J. Exp. Med. 161, 1–17. https://doi.org/10.1084/jem.161.1.1.

25. Sahin, U., Muik, A., Derhovanessian, E., Vogler, I., Kranz, L.M., Vormehr, M., Baum, A., Pascal, K., Quandt, J., Maurus, D., et al. (2020). COVID-19 vaccine BNT162b1 elicits human antibody and TH1 T cell responses. Nature 586, 594–599. https://doi.org/10.1038/s41586-020-2814-7.

26. Chung, Y.R., Dangi, T., Palacio, N., Sanchez, S., and Penaloza-MacMaster, P. (2022). Adoptive B cell therapy for chronic viral infection. Front. Immunol. 13, 908707. https://doi.org/10.3389/fimmu.2022.908707.

27. Bhattacharyya, M., Madden, P., Henning, N., Gregory, S., Aid, M., Martinot, A.J., Barouch, D.H., and Penaloza-MacMaster, P. (2017). Regulation of CD4 T cells and their effects on immunopathological inflammation following viral infection. Immunology 152, 328–343. https://doi.org/10.1111/imm.12771.

28. West, E.E., Youngblood, B., Tan, W.G., Jin, H.-T., Araki, K., Alexe, G., Konieczny, B.T., Calpe, S., Freeman, G.J., Terhorst, C., et al. (2011). Tight regulation of memory CD8(+) T cells limits their effectiveness during sustained high viral load. Immunity 35, 285–298. https://doi.org/10.1016/j.immuni.2011.05.017.

29. He, C., He, X., Yang, J., Lei, H., Hong, W., Song, X., Yang, L., Li, J., Wang, W., Shen, G., et al. (2022). Spike protein of SARS-CoV-2 Omicron (B.1.1.529) variant have a reduced ability to induce the immune response. Signal Transduct. Target. Ther. 7, 119. https://doi.org/10.1038/s41392-022-00980-6.

30. Lin, S., Chen, Z., Zhang, X., Wen, A., Yuan, X., Yu, C., Yang, J., He, B., Cao, Y., and Lu, G. (2022). Characterization of SARS-CoV-2 Omicron spike RBD reveals significantly decreased stability, severe evasion of

neutralizing-antibody recognition but unaffected engagement by decoy ACE2 modified for enhanced RBD binding. Signal Transduct. Target. Ther. *7*, 56. https://doi.org/10.1038/s41392-022-00914-2.

31. Zhang, J., Cai, Y., Lavine, C.L., Peng, H., Zhu, H., Anand, K., Tong, P., Gautam, A., Mayer, M.L., Rits-Volloch, S., et al. (2022). Structural and functional impact by SARS-CoV-2 Omicron spike mutations. Cell Rep. *39*, 110729. https://doi.org/10.1016/j.celrep.2022.110729.

32. Kim, W., Zhou, J.Q., Horvath, S.C., Schmitz, A.J., Sturtz, A.J., Lei, T., Liu, Z., Kalaidina, E., Thapa, M., Alsoussi, W.B., et al. (2022). Germinal centre-driven maturation of B cell response to mRNA vaccination. Nature *604*, 141–145. https://doi.org/10.1038/s41586-022-04527-1.

33. Turner, J.S., O'Halloran, J.A., Kalaidina, E., Kim, W., Schmitz, A.J., Zhou, J.Q., Lei, T., Thapa, M., Chen, R.E., Case, J.B., et al. (2021). SARS-CoV-2 mRNA vaccines induce persistent human germinal centre responses. Nature *596*, 109–113. https://doi.org/10.1038/s41586-021-03738-2.

34. Laidlaw, B.J., and Ellebedy, A.H. (2022). The germinal centre B cell response to SARS-CoV-2. Nat. Rev. Immunol. *22*, 7–18. https://doi.org/10.1038/s41577-021-00657-1.

35. Hawman, D.W., Meade-White, K., Archer, J., Leventhal, S.S., Wilson, D., Shaia, C., Randall, S., Khandhar, A.P., Krieger, K., Hsiang, T.Y., et al. (2022). SARS-CoV2 variant-specific replicating RNA vaccines protect from disease following challenge with heterologous variants of concern. Elife *11*, e75537. https://doi.org/10.7554/eLife.75537.

36. Reynolds, C.J., Pade, C., Gibbons, J.M., Otter, A.D., Lin, K.M., Muñoz Sandoval, D., Pieper, F.P., Butler, D.K., Liu, S., Joy, G., et al. (2022). Immune boosting by B.1.1.529 (Omicron) depends on previous SARS-CoV-2 exposure. Science *377*, eabq1841. https://doi.org/10.1126/science.abq1841.

37. Zhang, A., Stacey, H.D., Mullarkey, C.E., and Miller, M.S. (2019). Original antigenic sin: how first exposure shapes lifelong anti-influenza virus immune responses. J. Immunol. *202*, 335–340. https://doi.org/10.4049/jimmunol.1801149.

38. Hsieh, C.L., Goldsmith, J.A., Schaub, J.M., DiVenere, A.M., Kuo, H.C., Javanmardi, K., Le, K.C., Wrapp, D., Lee, A.G., Liu, Y., et al. (2020). Structure-based design of prefusion-stabilized SARS-CoV-2 spikes. Science *369*, 1501–1505. https://doi.org/10.1126/science.abd0826.

39. Pallesen, J., Wang, N., Corbett, K.S., Wrapp, D., Kirchdoerfer, R.N., Turner, H.L., Cottrell, C.A., Becker, M.M., Wang, L., Shi, W., et al. (2017). Immunogenicity and structures of a rationally designed prefusion MERS-CoV spike antigen. Proc. Natl. Acad. Sci. USA *114*, E7348–E7357. https://doi.org/10.1073/pnas.1707304114.

40. Ramadoss, N.S., Zhao, N.Q., Richardson, B.A., Grant, P.M., Kim, P.S., and Blish, C.A. (2020). Enhancing natural killer cell function with gp41-targeting bispecific antibodies to combat HIV infection. AIDS *34*, 1313–1323. https://doi.org/10.1097/QAD.0000000000002543.

41. Grunow, R., Franke, L., Hinkula, J., Wahren, B., Fenyö, E.M., Jondal, M., and von Baehr, R. (1995). Monoclonal antibodies to p24-core protein of HIV-1 mediate ADCC and inhibit virus spread in vitro. Clin. Diagn. Virol. *3*, 221–231. https://doi.org/10.1016/s0928-0197(94)00039-5.

42. Yang, Z., Liu, X., Sun, Z., Li, J., Tan, W., Yu, W., and Zhang, M. (2018). Identification of a HIV gp41-specific human monoclonal antibody with potent antibody-dependent cellular cytotoxicity. Front. Immunol. *9*, 2613. https://doi.org/10.3389/fimmu.2018.02613.

43. Dangi, T., Class, J., Palacio, N., Richner, J.M., and Penaloza MacMaster, P. (2021). Combining spike- and nucleocapsid-based vaccines improves distal control of SARS-CoV-2. Cell Rep. *36*, 109664. https://doi.org/10.1016/j.celrep.2021.109664.

44. Dangi, T., Palacio, N., Sanchez, S., Park, M., Class, J., Visvabharathy, L., Ciucci, T., Koralnik, I.J., Richner, J.M., and Penaloza-MacMaster, P. (2021). Cross-protective immunity following coronavirus vaccination and coronavirus infection. J. Clin. Invest. *131*, e151969. https://doi.org/10.1172/JCI151969.

45. Dangi, T., Chung, Y.R., Palacio, N., and Penaloza-MacMaster, P. (2020). Interrogating adaptive immunity using LCMV. Curr. Protoc. Immunol. *130*, e99. https://doi.org/10.1002/cpim.99.

46. Palacio, N., Dangi, T., Chung, Y.R., Wang, Y., Loredo-Varela, J.L., Zhang, Z., and Penaloza-MacMaster, P. (2020). Early type I IFN blockade improves the efficacy of viral vaccines. J. Exp. Med. *217*, e20191220. https://doi.org/10.1084/jem.20191220.

47. VanBlargan, L.A., Adams, L.J., Liu, Z., Chen, R.E., Gilchuk, P., Raju, S., Smith, B.K., Zhao, H., Case, J.B., Winkler, E.S., et al. (2021). A potently neutralizing SARS-CoV-2 antibody inhibits variants of concern by utilizing unique binding residues in a highly conserved epitope. Immunity *54*, 2399–2416.e6. https://doi.org/10.1016/j.immuni.2021.08.016.

48. Liu, Z., VanBlargan, L.A., Bloyet, L.M., Rothlauf, P.W., Chen, R.E., Stumpf, S., Zhao, H., Errico, J.M., Theel, E.S., Liebeskind, M.J., et al. (2021). Identification of SARS-CoV-2 spike mutations that attenuate monoclonal and serum antibody neutralization. Cell Host Microbe *29*, 477–488.e4. https://doi.org/10.1016/j.chom.2021.01.014.

49. Crawford, K.H.D., Eguia, R., Dingens, A.S., Loes, A.N., Malone, K.D., Wolf, C.R., Chu, H.Y., Tortorici, M.A., Veesler, D., Murphy, M., et al. (2020). Protocol and reagents for pseudotyping lentiviral particles with SARS-CoV-2 spike protein for neutralization assays. Viruses *12*, 513. https://doi.org/10.3390/v12050513.

50. Slifka, M.K., and Ahmed, R. (1996). Limiting dilution analysis of virus-specific memory B cells by an ELISPOT assay. J. Immunol. Methods *199*, 37–46. https://doi.org/10.1016/s0022-1759(96)00146-9.

STAR★METHODS

KEY RESOURCES TABLE

REAGENT or RESOURCE	SOURCE	IDENTIFIER
Antibodies		
αCD8, clone 53-6.7 in PerCPcy5.5	BD Pharmingen	Cat# 551162, RRID:AB_394081
αCD44, clone IM7 in Pacific Blue	Biolegend	Cat# 103020, RRID:AB_493683
αIFNγ, clone XMG1.2 in APC	BD Pharmingen	Cat# 554413, RRID:AB_398551
αCD4, clone RM4-5 FITC	eBioscience	Cat# 11-0042-82, RRID:AB_464896
Goat α mouse IgG-biotin, clone RM4-5 FITC	Invitrogen	Cat# SA5-10239, RRID:AB_2810197
Streptavidin (SA)-APC	Invitrogen	S868
biotin anti-mouse IgG1[a]	BD-Pharmingen	Cat# 553500, RRID:AB_394885
biotin anti-mouse IgG1[b]	BD-Pharmingen	Cat# 553533, RRID:AB_394903
anti-SARS-CoV-2 S protein (RBD epitope B), clone SARS2-34	BioXCell	Cat# BE0359, RRID:AB_2894778
anti-SARS-CoV-2 S protein (RBD epitope A), clone SARS2-01	BioXCell	Cat# BE0357, RRID:AB_2894776
Bacterial and virus strains		
Ad5-SARS CoV2 S	University of Iowa Vector Core, custom made	N/A
SARS-Related Coronavirus 2, Isolate USA-WA1/2020,	BEI resources	NR-52281
Chemicals, peptides, and recombinant proteins		
SARS CoV-2 S protein overlapping peptide pools (181 peptides)	BEI resources	NR-52402
SARS CoV-2 S protein for ELISA	Made by the Northwestern University recombinant protein production core using a SARS CoV-2 S protein gene provided by BEI (NR-52394, see above)	N/A
Critical commercial assays		
Quick RNA 96 kit (RNA extraction)	Zymo Research	R1052
Taqman RNA-to-CT step kit	ThermoFisher	4392653
Experimental models: Cell lines		
HEK-293	ATCC	CRL-1573
Vero-E6	ATCC	CRL-1586
Experimental models: Organisms/strains		
K18-hACE2 mice	Jackson Laboratories	034060
Recombinant DNA		
Plasmid containing SARS CoV-2 spike (S) gene	BEI resources	NR-52394
Software and algorithms		
GraphPad Prism software version 9.1.0	https://www.graphpad.com/scientific-software/prism/	N/A
FlowJo version 10.7.2	https://www.flowjo.com	N/A
Other		
K^{b}VL8 tetramer (APC)	Provided by the NIH tetramer core at Emory University	N/A
Forward primer, 5′ GACCCCAAAATCAGCGAAAT-3′	Integrated DNA Technologies	10006713

(Continued on next page)

Continued

REAGENT or RESOURCE	SOURCE	IDENTIFIER
Reverse primer, 5′ TCTGTTTACTGCCAGTTGAATCTG-3′	Integrated DNA Technologies	10006713
Probe, 5′ TCTGGTTACTGCCAGTTGAATCTG-3′	Integrated DNA Technologies	10006713
SARS CoV-2 copy number control	BEI resources	NR-52358
Live dead dye for flow cytometry	Invitrogen	L34976
Cytofix/cytoperm (fixing agent for flow cytometry)	BD Biosciences	554722
Phosphate buffer saline (PBS)	Gibco	14190-144
Golgi Plug	BD Biosciences	555029
Golgi Stop	BD Biosciences	554724
DMEM	Gibco	11965-092
Fetal bovine serum	Sigma	F0926-500

RESOURCE AVAILABILITY

Lead contact
Further information and requests for resources and reagents should be directed to and will be fulfilled by the lead contact Pablo Penaloza-MacMaster (ppm@northwestern.edu).

Materials availability
For mRNA vaccine access, contact Pablo Penaloza-MacMaster (ppm@northwestern.edu).

Data and code availability
All data reported in this paper will be shared by the lead contact upon request. This article does not report original code. Any additional information required to reanalyze the data reported in this paper is available from the lead contact upon request.

EXPERIMENTAL MODELS AND SUBJECT DETAILS

Animals and ethics statement
Mice were purchased from Jackson laboratories and were housed at Northwestern University or University of Illinois at Chicago (UIC) animal facility. All procedures were performed with the approval of the center for comparative medicine at Northwestern University and the UIC IACUC. Adult mice, approximately half females and half males, were used for the immunogenicity experiments included in this study. For the SARS-CoV-2 challenge studies, female mice were used.

In the human studies, all protocols used for participant recruitment, enrollment, blood collection, sample processing, and immunological assays with human samples were approved by the IRB of Northwestern University (STU00212583). All individuals voluntarily enrolled in the study by signing an informed consent form after receiving detailed information about the study. All volunteers self-identified as males or females, and were 18 years old or older.

METHOD DETAILS

Mice and vaccinations
6-8-week-old female K18-hACE2 mice were used for challenge studies, as done previously.[43] These mice express human ACE2 on the keratin 18 promoter. These mice were purchased from Jackson laboratories (Stock No: 034,860). Mice were immunized intramuscularly (50 μL per quadriceps) of mRNA-LNPs diluted in sterile PBS, as done previously.[43,44] All other experiments were performed with 6-8-week-old wild type mice (half males and half females) from Jackson laboratories (C57BL/6, Stock No: 000,664; or BALB/c, Stock No: 000651).

SARS-CoV-2 virus and infections
SARS-Related Coronavirus 2, Omicron Isolate was obtained through BEI Resources, NIAID, NIH: SARS-Related Coronavirus 2, Isolate hCoV-19/USA/MD-HP20874/2021 (Lineage B.1.1.529; Omicron Variant), NR-56461, contributed by Andrew S. Pekosz. This virus was propagated and tittered on Vero-E6 cells (ATCC). Vero-E6 cells were passaged in DMEM with 10% Fetal bovine serum (FBS) and Glutamax. Cells less than 20 passages were used for all studies. Virus stocks were expanded in Vero-E6 cells following a

low MOI (0.01) inoculation and harvested after 96 h. Titers were determined by plaque assay on Vero-E6 cell monolayers. Viral stocks were used after a single expansion (passage = 1) to prevent genetic drift. K18-hACE2 mice were anesthetized with isoflurane and challenged with 5×10^4 PFU of SARS-CoV-2 intranasally. Mouse challenges were performed at the University of Illinois at Chicago (UIC) following BL3 guidelines with approval by the UIC Institutional Animal Care and Use Committee (IACUC).

SARS-CoV-2 quantification in lungs
Lungs were isolated from infected mice and homogenized in sterile PBS. RNA was isolated with the Zymo 96-well RNA isolation kit (Catalog #: R1052) following the manufacturer's protocol. SARS-CoV-2 viral burden was measured by RT-qPCR using Taqman primer and probe sets from IDT with the following sequences: Forward 5′ GACCCCAAAATCAGCGAAAT-3′, Reverse 5′ TCTGGTT ACTGCCAGTTGAATCTG-3′, Probe 5′ ACCCCGCATTACGTTTGGTGGACC-3′. A SARS-CoV-2 copy number control was obtained from BEI (NR-52358) and used to quantify SARS-CoV-2 genomes.

Reagents, flow cytometry and equipment
Single cell suspensions were obtained from PBMCs or tissues. Dead cells were gated out using Live/Dead fixable dead cell stain (Invitrogen). MHC class I monomers (K^bVL8, VNFNFNGL) were used for detecting virus-specific CD8 T cells, and were obtained from the NIH tetramer facility located at Emory University. MHC monomers were tetramerized in-house. The VNFNFNGL epitope is located in position 539-546 of the SARS-CoV-2 spike protein. Cells were stained with fluorescently-labeled antibodies against CD8α (53-6.7 on PerCP-Cy5.5), CD44 (IM7 on FITC), CD127 (A7R34 on Pacific Blue), CD62L (MEL-14 on PECy7) and K^bVL8 (VNFNFNGL) tetramer (APC). Fluorescently labeled antibodies were purchased from BD Pharmingen, except for anti-CD127 and anti-CD44 (which were from Biolegend). Flow cytometry samples were acquired with a Becton Dickinson Canto II or an LSRII and analyzed using FlowJo v10 (Treestar).

SARS-CoV-2 spike and luciferase specific ELISA
Binding antibody titers were quantified using ELISA as described previously,[11,45,46] using the respective proteins as coating antigen. Briefly, 96-well, flat-bottom MaxiSorp plates (Thermo Fisher Scientific) were coated with 1 μg/mL of the respective protein for 48 h at 4°C. Plates were washed 3 times with wash buffer (PBS plus 0.05% Tween 20). Blocking was performed with blocking solution (200 μL PBS plus 0.05% Tween 20 plus 2% BSA) for 4 h at room temperature. 6 μL of plasma samples were added to 144 μL of blocking solution in the first column of the plate, 3-fold serial dilutions were prepared for each sample, and plates were incubated for 1 h at room temperature. Plates were washed 3 times with wash buffer. To determine mouse allotype-specific antibody (BALB/c or C57BL/6 derived), different primary antibodies were used: biotin anti-mouse IgG1[a] (BALB/c) specific antibody (BD-Pharmingen, MN 553500); or biotin anti-mouse IgG1[b] (C57BL/6) specific antibody (BD-Pharmingen, MN 553533). In the mAb therapy experiments, the mAb were of IgG1 isotype derived from BALB/c mice so we used biotin anti-mouse IgG1[a] specific antibody to quantify this mAb in the plasma of recipient mice. To quantify the endogenous antibody response in recipient mice that received mAb, we used biotin anti-mouse IgG1[b] combined with anti-mouse IgG2/IgG2b-specific antibody. Primary antibodies were diluted 1:1000 in blocking solution and were then added to the plates and incubated for 1 h at room temperature. Plates were washed 3 times with wash buffer and added streptavidin-HRP (Southern Biotech, 7105-05) diluted 1:400 in blocking buffer and incubated for 1 h at room temperature. After washing plates 3 times with wash buffer, 100 μL/well SureBlue Substrate (SeraCare) was added for 1 min. The reaction was stopped using 100 μL/well KPL TMB Stop Solution (SeraCare). Absorbance was measured at 450 nm using a Spectramax Plus 384 (Molecular Devices). Ancestral SARS-CoV-2 spike used in ELISAs was produced in-house using a plasmid produced under HHSN272201400008C and obtained from BEI Resources, NIAID, NIH: vector pCAGGS containing the SARS-related coronavirus 2; Wuhan-Hu-1 spike glycoprotein gene (soluble, stabilized); NR-52394. The ancestral receptor binding domain (RBD) protein used as coating antigen was made in-house; produced under HHSN272201400008C and obtained through BEI Resources (NIAID, NIH: Vector pCAGGS Containing the SARS-Related Coronavirus 2, Wuhan-Hu-1 Spike Glycoprotein Receptor Binding Domain (RBD), NR-52309. The Omicron RBD protein used as coating antigen was purchased from RayBiotech. The luciferase protein used as coating antigen was purchased from Sigma (L9420).

ADCC assays
ADCC assays were performed similar to our prior publication with a few modifications.[12] In brief, 293T cells were first transfected with the DNA used to in vitro transcribe the ancestral mRNA-spike vaccine to generate "target cells" expressing spike antigen. After 24-48 h, we confirmed spike protein expression on a fraction of the target cells by staining them with spike-specific mAbs[47,48] (clone SARS2-34 and SARS2-01 from BioXCell) conjugated to Alexa Fluor 647 for 30 min at 4°C. Cells were washed, fixed in 4% PFA, and analyzed on a Canto II flow cytometer (BD Biosciences). After confirming surface expression of spike protein, we utilized the rest of the live unstained cells as targets in ADCC assays. These cells expressing vaccine antigen (spike + targets) were co-cultured with NK effector cells expressing human CD16 (NK92.hCD16) or mouse CD16 (NK92.mCD16) at a 1:1 ratio (50,000 targets +50,000 effector NK cells) together with 1:20 diluted plasma in the presence of CD107a-FITC (Biolegend) and Golgi Plug/Golgi Stop (BD Biosciences). After 5 h the cultures were washed and stained with live/dead fixable dye and CD56-BV605 (Biolegend), followed by intracellular staining with IFNγ-APC (Biolegend). Cells were acquired on a Canto II flow cytometer. Quantification of target cell

killing was performed on a separate well without Golgi Plug/Golgi Stop. Effector NK92 cells expressing human or mouse CD16 (NK92.hCD16 and NK92.mCD16, respectively) were a kind gift from Drs. Oscar Aguilar and Lewis Lanier.

Surface binding of luciferase-specific antibodies from plasma

To examine binding of luciferase-specific plasma antibodies to the surface of luciferase + cells, 293T cells were transfected with the same DNA vector used for synthesizing the mRNA-luciferase. These cells were incubated with a 1:4 plasma dilution (naive versus luciferase-immune) for 1 h, followed by staining with goat anti-mouse IgG conjugated to Biotin (Catalog # SA5-10239, Invitrogen) for 30 min, followed by staining with SA-APC (Catalog #S868, Invitrogen) for 30 min. To assess intracellular binding, cells were first fixed with Cytofix/Cytoperm (BD Biosciences) and then permeabilized with 1x Perm Wash (BD Biosciences), followed by incubation with naive or luciferase-immune plasma (diluted in 1:4 in 1x Perm Wash) for 1 h, followed by staining with goat anti-mouse IgG conjugated to Biotin for 30 min, followed by staining with SA-APC for 30 min.

mRNA-LNP vaccines

We synthesized mRNA vaccines encoding for the codon-optimized SARS-CoV-2 spike protein from USA-WA1/2020 or Omicron BA.1. Constructs were purchased from Integrated DNA Technologies (IDT) or Genscript, respectively, and contained a T7 promoter site for *in vitro* transcription of mRNA. The sequences of the 5′- and -3′′-UTRs were identical to those used in a previous publication.[44] All mRNAs were encapsulated into lipid nanoparticles using the NanoAssemblr Benchtop system (Precision NanoSystems) and confirmed to have similar encapsulation efficiency (∼95%). mRNA was diluted in Formulation Buffer (Catalog # NWW0043, Precision NanoSystems) to 0.17 mg/mL and then run through a laminar flow cartridge with GenVoy ILM encapsulation lipids (Catalog # NWW0041, Precision NanoSystems) with N/P (Lipid mix/mRNA ratio of 4) at a flow ratio of 3:1 (RNA: GenVoy-ILM), with a total flow rate of 12 mL/min, to produce mRNA–lipid nanoparticles (mRNA-LNPs). mRNA-LNPs were evaluated for encapsulation efficiency and mRNA concentration using RiboGreen assay using the Quant-iT RiboGreen RNA Assay Kit (Catalog # R11490, Invitrogen, Thermo Fisher Scientific). mRNA to express luciferase was purchased from TriLink Biotechnologies (CleanCap FLuc mRNA, L-7602, CleanCapFirefly Luciferase) and was encapsulated into lipid nanoparticles using the aforementioned protocol.

In vivo bioluminescence

Mice were imaged at various times after immunization. To quantify luciferase expression, luciferin (GoldBio, Catalog # LUCK-100; weight of 10 μL/g) was administered intraperitoneally 15 min before imaging. Mice were anesthetized and imaged for 45 s using a SII Lago IVIS Imager (Spectral Instruments Imaging). Region of interest (ROI) bioluminescence was used to quantify signal. Each leg (quadriceps) was treated as an individual site of immunization (or individual data point).

Pseudovirus neutralization assays

SARS-CoV-2 pseudovirus neutralization assays were performed as described previously.[11,49] In brief, we utilized a SARS-CoV-2 spike pseudotyped lentivirus kit obtained through BEI Resources, NIAID, NIH (SARS-Related Coronavirus 2, Spike-Pseudotyped Lentiviral Kit V2, NR-53816). We used HEK-293T–hACE2 cells as targets (BEI Resources, NIAID, NIH, NR-52511). Serial plasma dilutions were incubated with the SARS-CoV-2 spike pseudotyped lentivirus (ancestral or Omicron BA.1). Cells were then lysed using luciferase cell culture lysis buffer (Promega). The reaction was added to 96-well black optiplates (PerkinElmer) and luminescence was quantified using a PerkinElmer Victor3 luminometer.

B cell ELISPOT

Antibody secreting cells (ACS) were enumerated similar to a prior paper, but using spike protein as coating antigen instead of viral lysate.[45] In brief, SARS-CoV-2 spike-specific ASC were quantitated by ELISPOT using 96-well Multiscreen filter plate (MSHAN4B50, Millipore Ireland BV). Plates were coated with 5 μg/mL of the SARS-CoV-2 spike protein and incubated overnight at 4°C. After incubation, plates were washed once with PBS containing 0.05% Tween 20 (PBS-T) and twice with PBS. Plates were blocked by incubating plates with RPMI containing 10% fetal bovine serum (FBS) for 2 h at room temperature. Single suspensions of bone marrow cells at 60×10^6 cells/mL were prepared in medium (RPMI supplemented with 10% FBS, 1% penicillin/streptomycin, and 1% L-glutamine and 0.05 mM of B-Mercaptoethanol). After incubation, blocking medium was replaced with 100 μL/well of fresh medium and added 50 μL of single cell suspension to the first row, and serially diluted 3-fold down the plate. Plates were incubated for 8 h at 37°C in a 5% CO_2 incubator. Plates were washed with PBS and PBS-T, and incubated with 100 μL of biotinylated anti-mouse IgG antibody diluted 1:1000 in PBS-T with 1% FBS for two days at 4°C. Antibody was removed by flicking plates followed by washing four times with PBS-T, and 100 μL of horseradish peroxidase (HRP) conjugated avidin D (A-1004, Vector Laboratories, Burlingame, CA) was added per well at 5 μg/mL in PBS-T with 1% FCS and incubated for 1 h at room temperature. Plates were washed three times with PBS-T and PBS before adding 100 μL of freshly prepared chromogen substrate. The substrate was prepared by adding 0.15 mL of AEC solution (3-amino-9-ethyl carbazole, MP Biochemical#195039) at a concentration of 20 mg/mL in dimethylformamide (Sigma, St. Louis, MO) to 10 mL of 0.1M sodium acetate buffer (pH = 4.8). This solution was filtered through a 0.2 μm membrane and 100 μL of 3% H_2O_2 was added immediately before use. Plates were incubated with substrate for 8 min until spots appeared and the reaction was stopped by rinsing plates with water. Plates were allowed to dry and spots were counted. Memory B cells were enumerated in mouse spleen as described previously using feeder cells,[50] but instead of using viral lysate we used SARS-CoV-2 spike protein as coating antigen.

IgG purification from plasma and generation of F(ab')2 fragments

Naive plasma and immune plasma were harvested. IgG was purified from whole plasma using a protein G chromatography column (Cytiva, Catalog # 29048581). To generate F(ab')2 fragments, purified IgG was digested with pepsin using the Pierce F(ab')2 preparation kit (Thermo Fisher, Catalog # 44988). Undigested IgG was removed by protein A purification, and protein concentration was measured at 280 nm absorbance on a nanodrop (Thermo Fisher). Complete digestion of IgG was confirmed by running a non-reducing SDS-PAGE gel (Biorad, Catalog # 4561095). Undigested IgG or digested IgG were mixed with Laemmli sample buffer (Biorad) in a non-reducing environment, followed by separation in a polyacrylamide gel followed by staining with Coomassie Brilliant Blue R-250. 1000 μg of purified IgG or F(ab')2 were injected intraperitoneally into mice, and on the following day, mice received mRNA vaccines intramuscularly.

Comparing spike protein expression by ancestral and Omicron vaccines

293T cells were transfected with pcDNA3.1 vectors expressing ancestral or Omicron spike protein (same vectors used for generating mRNA-spike vaccines). After 1 day, we confirmed spike protein expression on the surface of 293T cells, by staining cells with spike-specific mAbs (clone SARS2-34 and SARS2-01)[47,48] conjugated to Alexa Fluor 647 for 30 min at 4°C. Cells were washed, fixed in 4% PFA, and analyzed on a Canto II flow cytometer (BD Biosciences).

QUANTIFICATION AND STATISTICAL ANALYSIS

The number of data points in some figures varies due to sample availability or logistical reasons. For example, the ELISAs use only 5 μL of plasma, whereas the neutralization assays use 20 μL of plasma, so we were able to perform ELISAs in more experiments. Since immunogenicity studies do not require BSL-3, we were able to perform more immunogenicity studies than challenge studies (Figure S4). Statistical analyses are indicated on the figure legends. Statistical significance was established at p ≤ 0.05. Data were analyzed using Prism (Graphpad).